

# Abstract

# Contents

<b>1</b>	<b>Introduction</b>	<b>1</b>
<b>2</b>	<b>Theoretical background</b>	<b>6</b>
2.1	Continuum electro-elasticity . . . . .	6
2.2	Entropy-driven electro-elasticity of an isotropic polymer network . . . . .	9
2.3	Phenomenological approach to electro-elasticity . . . . .	13
<b>3</b>	<b>Electro-elasticity of solutions and anisotropic networks of polymer molecules</b>	<b>15</b>
3.1	First law of thermodynamics . . . . .	15
3.2	<del>One-dimensional</del> $\mathbf{H-D}$ systems of charges, dipoles, and molecular chains in an electric field . . . . .	15
3.2.1	A single electric charge . . . . .	16
3.2.2	Dipoles . . . . .	17
3.2.3	Polymer molecule (chain) . . . . .	20
3.3	Polymer molecules (chains) in electric field . . . . .	24
3.3.1	<del>Monomers orientational</del> $\mathbf{d}$ Distribution of monomer orientation . . . . .	24
3.4	An anisotropic network of polymer molecules . . . . .	25
3.4.1	Deriving the properties of the polymer . . . . .	30
<b>4</b>	<b>Application to electrostatically biased network</b>	<b>33</b>
4.1	Chains distribution . . . . .	33
4.2	Monomers orientation . . . . .	36
4.3	The free state . . . . .	38
4.4	<del>M</del> $\mathbf{T}$ he materials properties . . . . .	40
4.5	The coupled response . . . . .	41
<b>5</b>	<b>Experimental work</b>	<b>43</b>
5.1	<del>The</del> $\mathbf{i}$ nfluence of uniaxial and biaxial stretching . . . . .	43
5.2	<del>I</del> $\mathbf{T}$ he influence of an electric field . . . . .	45
5.2.1	Experimental set-up . . . . .	45
5.2.2	Results and discussion . . . . .	47
<b>6</b>	<b>Conclusions</b>	<b>49</b>
	<b>References</b>	<b>53</b>
<b>A</b>	<del>Presentation of</del> $\mathbf{t}$ $\mathbf{T}$ he first law of thermodynamics in terms of <del>electrical</del> <del>enthalpy</del> electric enthalpy	<b>54</b>

B Chain stress and deriving the chain end-to-end vector <del>by</del> from the deformation gradient	57
C The initial guess for $\tau$	58

# List of Figures

1	A schematic description of the coordinate system $\{\hat{\mathbf{E}}, \hat{\mathbf{Y}}, \hat{\mathbf{Z}}\}$ and the applied spherical coordinates. . . . .	9
2	Schematic description of an arbitrary one dimensional system subjected to electromechanical excitation at its boundary. . . . .	15
3	Schematic description of a single charge subjected to an electric field. . . .	16
4	Schematic description of a single dipole consisting of two charges, $Q^+$ and $Q^-$ , connected by a stiff rod in an electric field. . . . .	17
5	Schematic description of a dipole in an electric field. . . . .	19
6	The entropy of a polymer chain with uniaxial dipoles as a function of the normalized radius as $0 \leq \frac{r}{nl} \leq 1$ and $l = 100 \mu\text{m}$ . The red continuous curve with circular markers corresponds to $n = 50$ and the brown curve with squares to $n = 100$ . The dashed columns corresponds to the normalized radii in accordance with the results in section 3.2.3, $\frac{r}{nl} = \sqrt{\frac{2}{3}} \frac{1}{\sqrt{n}}$ , and the dot-dashed columns to the results from random walk statistics, $\frac{r}{nl} = \frac{1}{\sqrt{n}}$ . . . . .	35
7	The natural logarithm for the maximum number of configurations as a function of the electric field magnitude for chains with uniaxial dipoles at different inclinations. The blue curve with circular markers corresponds to $\Theta = \frac{\pi}{1000}$ , the red curve with squares to $\Theta = \frac{\pi}{4}$ and the yellow curve with diamonds to $\Theta = \frac{\pi}{2}$ . . . . .	35
8	The most probable end-to-end length as a function of the electric field magnitude for chains with uniaxial dipoles at different inclinations. The blue curve with circular markers corresponds to $\Theta = \frac{\pi}{1000}$ , the red curve with squares to $\Theta = \frac{\pi}{4}$ and the yellow curve with diamonds to $\Theta = \frac{\pi}{2}$ . . . . .	35
9	The size of the Lagrange multiplier $\tau$ , associated with the most probable radius as a function of the electric field magnitude for chains with uniaxial dipoles at different inclinations. The blue curve with circular markers corresponds to $\Theta = \frac{\pi}{1000}$ , the red curve with squares to $\Theta = \frac{\pi}{4}$ and the yellow curve with diamonds to $\Theta = \frac{\pi}{2}$ . . . . .	36
10	The monomer distribution for a polymer chain of uniaxial dipoles. The magnitude of the electric field during the polymerization process is $E = 150 \frac{\text{MV}}{\text{m}}$ . (a) Corresponds to the chain with the inclination $\Theta = \frac{\pi}{1000}$ and end-to-end length $r = 0.89 \sqrt{n} l$ . (b) Corresponds to $\Theta = \frac{\pi}{4}$ and $r = 0.91 \sqrt{n} l$ . (c) Corresponds to $\Theta = \frac{\pi}{2}$ and $r = 0.93 \sqrt{n} l$ . . . . .	37
11	The amorphous monomer distribution of a uniaxial dipole as $E = 150 \frac{\text{MV}}{\text{m}}$ . According to the numerical analysis as $\tau = 0$ and identical to the results of the analytical analysis that was presented by ?. . . . .	37

12	The number of chains along each inclination as a function of the inclination relative to the direction of the electric field, $N(\Theta, \Phi = 0)$ . The blue curve with circular markers corresponds to the isotropic polymer and the yellow curve with squares corresponds to the biased polymer. . . . .	38
13	The fractions of chains along each inclination as a function of the inclination to the direction of the electric field, $\nu(\Theta)$ . The blue curve with circular markers corresponds to the isotropic polymer and the yellow curve with squares corresponds to the biased polymer. . . . .	38
14	$\sigma_{\text{Diff}} = \sigma_{\text{EE}} - \sigma_{\text{YY}}$ as a function of $\lambda_0$ after the removal of the electric field with the magnitude of $E = 150 \frac{\text{MV}}{\text{m}}$ . . . . .	40
15	The deviatoric mechanical stress as a function of the deformation ratio, $\lambda$ . Dashed curves corresponds to the isotropic polymer, continuous curves to the biased polymer and the dot-dashed curves to a polymer described by the IED model. The blue curves corresponds to the normal stress in the direction of the electric field, $\sigma_{\text{EE}}^{\text{m}}$ , and the red curves to the transverse stress, $\sigma_{\text{YY}}^{\text{m}} = \sigma_{\text{ZZ}}^{\text{m}}$ . . . . .	40
16	The susceptibilities of the polymers as a function of the electric field. The black dashed curve corresponds to the isotropic polymer, the black continuous curve to the biased polymer and the black dot-dashed line to a polymer described by the IED model. (the dashed and the continuous curves overlap).	41
17	The deformation in the direction of the electric field, $\lambda$ , as a function of the magnitude of the electric field. The black dashed curve corresponds to the isotropic polymer, the black continuous curve to the biased polymer and the black dot-dashed curves to a polymer described by the IED model. . .	42
18	(a) The self constructed stretching device. (b) The C-clamp used as a parallel plate capacitor. . . . .	44
19	The relative permittivity measurements as functions of the percentage of surface area expansion. The dashed and dotted curves correspond to the analytical results [?], as $n$ are estimated from the stretch at failure ( $n_f$ ) and from fitting the analytical equations to the experimental results ( $n_e$ ), respectively. (a) PDMS under uniaxial stretch. (b) VHB under uniaxial stretch. (c) VHB under biaxial stretch. . . . .	44
20	A schematic description of the experimental system. . . . .	46
21	The parts of the plate capacitore. . . . .	46
22	The permittivity measurements a functions of the electric field on the sample. The Blue dots corresponds to a relaxed sample and the red circles corresponds to the area pre-stretch of $A = 225\%$ . (a) PDMS, (b) VHB. . .	47

## List of Tables

- 1 The number of monomers in a single chain for the case presented in Fig. 19. 45

# 1 Introduction

(Note: Strong points for EAP use)

Dielectric elastomers (DEs) are polymers that are nonconductive but polarize and deform under electrostatic excitation. These lightweight and flexible polymers are readily available and may potentially be used as actuators in a wide variety of applications such as artificial muscles, energy-harvesting devices, micropumps, and soft robotics [?].

(Note: The microstructure and macrostructure of the EAP (polymer networks from chains and chains from monomers -> a polymer strip sandwiched between two electrodes))

At the microscopic level, DEs have a hierarchical structure of polymer-chain networks. A polymer chain is a long string of repeating dipolar monomers. At the macroscopic level, the essential part of a DE-based device is a thin, soft DE membrane sandwiched between two compliant flexible electrodes. When an electric potential is applied across the electrodes, the monomers react to the electric excitation while the DE membrane becomes thinner as a result of the attraction between the two oppositely charged electrodes. Simultaneously, the membrane area expands due to the Poisson's effect. This process converts electrical energy into mechanical energy. The attractive features of dielectric elastomers include large strain, fast response, silent operation, low cost, and high efficiency [?].

(Note: The ratio between elastic moduli and dielectric moduli and its importance)

The electromechanical coupling in DEs is characterized by a quadratic dependence of the force between the electrodes on the applied electric potential [?]. In turn, the deformation depends on the force via the elastic moduli. Thus, the coupling depends on the ratio between the dielectric and the elastic moduli. Commonly, flexible polymers typically have low dielectric moduli, whereas polymers with high dielectric moduli are generally stiff. Given that this ratio is relatively small, large electric potentials are needed to obtain non-negligible actuation.

(Note: electric breakdown and other failure mechanisms)

The requirement for high electric potentials implies that the feasibility of these materials is limited by their dielectric strength, which is the limit electric potential beyond which electric current flows through the dielectric material [?]. Exceeding this electric potential results in what is known as electric breakdown or dielectric breakdown. In some cases, this results in a transformation of the insulator into an electric conductor. In general, dielectric breakdown may be a singular, a cyclic, or a continuous event [?]. Accurately predicting the occurrence of an electrical breakdown and its timing and position, is not yet possible, essentially mostly because it does not depend on a single cause, but it is a statistical product of several factors. The most notable factors are the local defects, such as voids or inclusions that would create a

locally decrease ~~in the thickness of~~ the DE thickness, ~~leading to higher~~ increasing the local electric fields and/or higher mechanical stresses [?]. In practice, the dielectric strength is measured experimentally [??] ~~and is measured~~ for a membrane ~~withat~~ a given thickness and with ~~a given~~ the requisite testing equipment [?]. ~~In their work~~ ?? examined the failure mechanisms and the performance boundaries of DEs ~~and~~. ~~Their analysis~~ showed that the performance ~~of DEs made with~~ of highly viscoelastic polymer membranes as DEs is governed by four key mechanisms ~~which are~~: dielectric breakdown, current leakage, pull-in failure, and viscoelasticity.

(Note: The ratio between elastic moduli and dielectric moduli - low but can be improved)

~~A~~One possible way to overcome ~~the dielectric breakdown failure mechanism~~ is by reducing the electric potentials ~~that are~~ currently ~~needed~~required for ~~a meaningful~~non-negligible actuation, ~~this~~which can be done by improving the DE polarizability ~~of the DE~~. Several previous works suggest that the low ratio ~~between of the~~ dielectric ~~and~~modulus to ~~the~~ elastic modulus ~~i~~ may be improved, ~~which would and thus their~~enhance the electromechanical response ~~may be enhanced~~. A common ~~general~~ approach ~~for to~~ improving this ratio involves inserting additional materials ~~into~~ the elastomer. This approach can result in a homogeneous or ~~a~~ composite elastomer. One aspect of ~~the is~~ approach ~~refers to~~involves embedding ~~materials into soft polymer~~ components with a higher dielectric constant, ~~which (i.e., that can be classified as insulating or conducting), in a soft polymer~~ [????]. ? presented such a method ~~for to enhance~~ the electromechanical response ~~enhancement~~ of silicone elastomer networks, ~~based on the~~ by grafting ~~of~~ molecules with high permanent dipoles to the crosslinking ~~er~~ molecules. Through adjusting the crosslinking density, their method also ~~allows for~~~~aprovides~~ direct control of the mechanical properties of the elastomer ~~by adjustments of the crosslinking density~~. Another aspect of the approach ~~refers to~~involves improving the actuation in DEs ~~with an~~by appropriately adjust~~ment of~~ing their microstructure as periodic laminates [?????].

(Note: improving the response without changing the ratio between elastic moduli and dielectric moduli)

~~As a contrary to~~In contrast with the approach of improving the ratio ~~between the of~~ dielectric modulus ~~and to~~ elastic modulus ~~i~~, several works, ~~which mainly target soft robotics,~~ have ~~been done~~chosen to improve the responsiveness of DEs by adjusting the macroscopic structure of the actuators. ~~These works are mainly in regards to soft robotics, but not limited to it~~ [????]. Recent works, such as ? and ? ~~have~~ discussed soft electrohydraulic transducers, ~~termed~~which are called “Peano-HASEL (~~hydraulically amplified self-healing electrostatic~~)-actuators.” (hydraulically amplified self-healing electrostatic actuators). Such actuators combine the ~~strengths~~advantages of both fluidic actuators and electrostatic actuators. ~~This combination is performed as the actuators and~~ are comprised of pouches, ~~which are~~ made of flexible dielectric polymer films, filled with a liquid dielec-

tric and covered with compliant electrodes. ~~When~~ Upon applying a voltage ~~is applied to~~ across the electrodes, they “zip” together ~~due to~~ because of ~~the~~ Maxwell stress, which ~~causes~~ displaces the liquid inside the pouch ~~to be displaced~~, and ~~thus causes the~~ thereby contraction ~~of~~ the actuator [?].

(Note: Previous investigations of the polymer properties:)

(Note: Mechanical response)

The ~~aspiration to affect~~ desire to adjust the DE ratio ~~between the~~ of dielectric modulus ~~and~~ to elastic modulus ~~of DEs~~ motivates a multiscale inquiry of ~~their~~ the mechanical, dielectric, and coupled properties ~~of these materials~~. The response of polymers to purely mechanical loading across all scales ~~was~~ has been extensively investigated ~~extensively~~. For example, ~~A~~ investigated in detailed ~~investigation of~~ the macroscopic behavior of soft materials undergoing large deformation ~~is presented in~~ ?. ? used statistical mechanics to make ~~a~~ a pioneering analysis at the microscopic level ~~was performed through the use of statistical mechanics by~~ ?, which resulted in a Langevin-based constitutive relation. This work led to a variety of multiscale models, such as the three-chain model [?] and the eight-chain model [?]. ~~Such an~~ A similar analysis of mechanical systems was also presented by ?, ?, and ? for ~~polymer networks with~~ rubberlike elasticity ~~of polymer networks~~. A ? review ~~of~~ the development of statistical-mechanics treatments of rubber elasticity, ~~and was given in~~ ?. ? and ? ~~presented an use~~ statistical mechanics to ~~analysis of~~ the mechanical systems ~~through the use of statistical mechanics for~~ of liquid-crystal elastomers.

(Note: Electrostatic response)

? and ?, among others, extensively examined ~~t~~ The response of polymers to electrostatic excitation ~~was examined extensively at~~ on the macroscopic and microscopic scales. ~~by ? and ? among others.~~ ~~D~~ They ~~discussing~~ and ~~analyzing~~ the constitutive relations for the macroscopic electric parameters, such as ~~the~~ polarization and ~~the~~ displacement, and for the microscopic electric parameters, such as the dipoles ~~moments~~ and the bound and free charge densities. In other work, ? presented an electrostatic theory for rigid bodies as ~~ideal~~ theoretical ~~ideal~~ constructs ~~while executing histo~~ analyze ~~analysis from~~ a single charges to a continuum of charge.

(Note: Coupled response)

? ~~was the first to~~ The ~~analysis~~ ~~of~~ the coupled electromechanical response of DEs at the macroscopic level ~~began with the work of~~ ?. Years later, ? introduced ~~an invariant-based representation to study~~ the constitutive behavior of electro-sensitive elastomers ~~via an invariant-based representation, and~~. ~~t~~ This work was expanded to ~~the class of~~ anisotropic materials by ?. Among others, ? and ? investigated ~~the influence of the~~ how deformation and the rate of deformation ~~on~~ affected ~~the~~ electromechanical coupling. ~~At the macroscopic level,~~ ? ~~performed an~~ analyzed ~~sis at the macroscopic level for~~ the electromechanical response of membranes under a uniaxial force, under equal-biaxial forces,

and for ~~the case of~~ a membrane constrained in one direction and subject to a force in the ~~other opposite~~ direction. ~~Additionally~~ Additionally, they examined the response of a fiber-constrained membrane. ~~?~~ presented a principle of virtual work for problems ~~of involving~~ combined electrostatic and mechanical loading, ~~which and that~~ includes the interactions between the resulting strain and polarization, ~~was presented by ?~~. Physically motivated multiscale analyses of ~~the~~ electromechanical coupling were ~~previously performed~~ done by ?, ?, and ?, and ~~?~~ introduced ~~m~~ Multiscale analysis ~~that was~~ based on statistical mechanics ~~was introduced by ?~~.

(Note: Experimental work)

In addition to the ~~discussed~~ theoretical works, ~~over the past 20 years~~ the dielectric properties of DEs have been extensively investigated experimentally ~~over the past two decades~~. Although ~~some have determined~~ the variation in the relative permittivity of DEs, such as VHB 4910/4905, ~~has been determined~~ under ~~conditions of negligible~~ biaxial extension ~~to be negligible, as can be seen in the works of~~ (see, e.g., ? and ~~?~~ among others), ~~several other~~ works have contradicted ~~these~~ conclusions. Several investigations ~~on the variation of~~ have revealed a decrease in the relative permittivity ~~as a result of~~ with increasing area ~~stretch have revealed a decrease in its value~~. For example, ? measured an initial relative permittivity  $\epsilon_r = 4.4$  ~~and versus~~  $\epsilon_r = 2.25$  ~~under~~ for a ninefold area stretch of 9, and ~~?~~ measured  $\epsilon_r = 4.68$  ~~and versus~~  $\epsilon_r = 2.62$  ~~as the initial relative permittivity and under~~ for a 25-fold area stretch of 25, respectively. In addition, ? measured ~~a decrease as well while performing a planar stretch of 16, as an initial permittivity~~  $\epsilon_r = 4.36$  ~~was the initial permittivity and versus~~  $\epsilon_r = 2.44$  ~~was the measurement under stretch~~ for a 16-fold planar stretch. ? found ~~from their~~ experimentally ~~work on~~ from the electromechanical response of ~~the~~ polyurethane elastomer that ~~the chain motions of chains~~ can be divided into ~~those motion~~ related to the mechanical response and ~~those motion~~ related to the polarization response, ~~while and that~~ the overlap between ~~them~~ these motions yields the electromechanical response. ~~Some~~ Other experimental works, such as ?, ?, and ?, examined ~~biaxially and uniaxially prestrained silicone and acrylic elastomers to study how the influence of prestraining the DEs membranes on affects the actuator performance of actuators. These examinations were performed for biaxially and uniaxially prestraining silicone and acrylic elastomers. Furthermore, some~~ Finally, work has been done ~~into~~ developing models ~~that assist in~~ for estimating the variation in relative permittivity as a ~~result of different~~ function of various stretch combinations [??]. An example of such work is ~~the one presented was done by in~~ ?, ~~where~~ who compared the results of a statistical-mechanics-based model ~~is compared to~~ with experimental findings.

(Note: This work)

(Note: A brief description of the displayed content)

We begin this work ~~with a~~ by discussing the theoretical background, within the frame-

work of a continuum approach and considering, concerning the mechanical, electrostatic, and coupled cases. Following are a Next, we review of the analysis of the microstructure of an isotropic polymer chain network by using statistical mechanics throughwith entropy considerations and amake reference ofto a phenomenological model for the electromechanical coupling of DEs that will be compared totested against our experimental results. In sSection 3-an analyzessis-of the DEs electro-elasticity in several hierarchical cases, ranging from a single electric charge to a network, is-presented. MoreoverIn addition, we discuss the means of assessing the structure and properties of a general polymer-will-be-discussed. Section 4 deals-withpresents a numerical application of the electrostatically biased polymer network.-This to demonstrates the influence-of performing thehow polymerization process-ofing a polymer under an electric field,-on affects the structure of the polymer network and it's properties,-all-while-comparing. This work is done by comparing the electric-field-polymerized polymer it-to an isotropic polymer network and to the results of the phenomenological model. Next,-our experimental work is-presented-in-sSection 5 presents our experimental work, which is-meant-to gives an additional perspective thanon our theoretical work. The experimental work includes an evaluation of the-influence-ofhow uniaxial and biaxial stretching of DEs on-affects their dielectric constant. Moreover, we introduce a new experimental system whichthat allows us to evaluate the-variations-inhow the dielectric constant of DEs at-different-magnitudes-ofon the electric-field magnitudes. Finally, the conclusions are gathered in sSection 6.

## 2 Theoretical background

(Note: Multiscale entropy based analysis)

The mechanical and electrostatic energy balance is formulated in terms of the electric enthalpy. The analyses will be carried out by taking into account the entropy of the chains network within the framework of statistical mechanics with the appropriate kinematic and energetic constraints.

### 2.1 Continuum electro-elasticity

(Note: basic continuum mechanics - mechanics aspect)

Consider an electro-elastic solid continuum in a stress-free configuration in the absence of electric field and mechanical load. Let material particles be labelled by their position vector  $\mathbf{X}$  in this referential configuration. In the deformed configuration, the point  $\mathbf{X}$  occupies the position  $\mathbf{x} = \chi(\mathbf{X}, \mathbf{t})$ , where the vector field  $\chi$  describes the deformation of the material. We require  $\chi$  to be a one-to-one, orientation-preserving, and twice continuously differentiable mapping [?].

(Note: continuum mechanics - mechanics)

The deformation gradient tensor is

$$\mathbf{F} = \nabla_{\mathbf{X}}\chi(\mathbf{X}, \mathbf{t}), \quad (1)$$

where  $\nabla_{\mathbf{X}}$  is the gradient operator and the subscript  $\mathbf{X}$  implies that the derivatives are taken with respect to the referential coordinate system. The Cartesian components of  $\mathbf{F}$  are  $F_{ij} = \frac{\partial x_i}{\partial X_j}$ , where  $X_i$  and  $x_i$  ( $i = 1, 2, 3$ ) are the Cartesian components of  $\mathbf{X}$  and  $\mathbf{x}$ , respectively.  $J \equiv \det(\mathbf{F})$  is the ratio between volume elements in the current and reference configurations, with the convention of being strictly positive. Moreover, the velocity of the material points is  $\mathbf{v}(\mathbf{x})$  and accordingly, the spatial velocity gradient is

$$\mathbf{L} = \nabla_{\mathbf{x}}\mathbf{v} = \dot{\mathbf{F}}\mathbf{F}^{-1}, \quad (2)$$

where  $\nabla_{\mathbf{x}}$  is the gradient operator taken with respect to the current coordinate system.

(Note: continuum mechanics - electrostatic)

The body is subjected to an electric field  $\mathbf{E}(\mathbf{x})$ , which satisfies the relation  $\nabla_{\mathbf{x}} \times \mathbf{E}(\mathbf{x}) = 0$  in the entire space. The electric potential  $\phi$  is a scalar quantity defined such that  $\mathbf{E} = -\nabla_{\mathbf{x}}\phi$ . The electric induction, also known as the electric displacement, is

$$\mathbf{D}(\mathbf{x}) = \epsilon_0 \mathbf{E}(\mathbf{x}) + \mathbf{P}(\mathbf{x}), \quad (3)$$

where the constant  $\epsilon_0$  is the vacuum permittivity ~~of vacuum~~ and  $\mathbf{P}(\mathbf{x})$  is the electric ~~dipole density~~, also known as the polarization ~~in vacuum~~ ( $\mathbf{P} = 0$  in vacuum). The electric displacement in ideal dielectrics or in a continuum with no free charges is governed by ~~the equation~~

$$\nabla_{\mathbf{x}} \cdot \mathbf{D}(\mathbf{x}) = 0. \quad (4)$$

(Note: continuum mechanics - the electromechanical coupling)

The electrical boundary conditions for the electromechanical problem are given in terms of the electric potential or the charge per unit area ~~on the boundary~~  $\rho_a$  ~~on the boundary~~, which is the charge on the electrodes such that  $\mathbf{D} \cdot \hat{\mathbf{n}} = -\rho_a$ , where  $\hat{\mathbf{n}}$  is the outer ~~pointing~~ unit vector normal to the boundary in the current configuration. The mechanical boundary conditions are stated in terms of the displacement or the mechanical traction  $\mathbf{t}$ . The electric field in the surrounding space induces a Maxwell's stress

$$\boldsymbol{\sigma}^M = \epsilon_0 \left( \mathbf{E} \otimes \mathbf{E} - \frac{1}{2}(\mathbf{E} \cdot \mathbf{E})\mathbf{I} \right). \quad (5)$$

Accordingly, the traction boundary condition is  $(\boldsymbol{\sigma} - \boldsymbol{\sigma}^M) \hat{\mathbf{n}} = \mathbf{t}$ . Assuming no body forces, the stress that develops in a dielectric  $\boldsymbol{\sigma}$  due to the electromechanical loading satisfy the equilibrium equation

$$\nabla_{\mathbf{x}} \cdot \boldsymbol{\sigma} = 0. \quad (6)$$

(Note: The first law of thermodynamics - energy balance)

~~A~~The balance of energy is formulated ~~throughby applying~~ the first law of thermodynamics:

$$\frac{dU}{dt} = \frac{dW}{dt} + \frac{dQ}{dt}, \quad (7)$$

where  $U$  represents the internal energy stored in the material,  $W$  is the work ~~ofdone on the system by~~ any external sources, mechanical ~~andor~~ electrical, and  $Q$  ~~denotesis~~ the ~~quantity of~~ energy supplied to the system as heat. Following ?? and ?, a Legendre transform ~~ofis applied to~~ the internal energy ~~is used in order~~ to formulate the energy balance in terms of the electric ~~enthalpy density~~:  $H = U - \mathbf{J}\mathbf{P} \cdot \mathbf{E}$ . ~~In order to~~ To formulate the energy balance in terms of entropy, which relates to the ~~systems~~ number of microscopic configurations ~~of the system~~, we refer to a polymer as a reversible or conservative material [?]; (i.e., a material that does not absorb the work done by external agents but stores it as dielectric polarization or elastic deformation). ~~HenceThus~~, following the Clausius theorem ~~in the case of~~ for a reversible material or system, the entropy change is ~~defined as~~  $dS = \frac{dQ}{T}$ , where  $S$  is the entropy-density ~~function~~ per unit referential volume and  $T$  is the absolute temperature. Thus, ~~while~~ taking into account the analysis presented in appendix A [?], we consider a general representation in which the first law of thermodynamics ~~istakes the~~

form

$$\dot{H}^r - \frac{d}{dt} \int_{\mathbb{R}^3} \frac{\epsilon_0}{2} \mathbf{E} \cdot \mathbf{E} dV = \dot{W}^r + T \dot{S}^r, \quad (8)$$

where we consider an electro-elastic system  $\mathcal{Y} \subset \mathbb{R}^3$ .

~~In the work of ? gives, at the following~~ specific representation of Eq. (8) ~~was presented for the to~~ analyze ~~of~~ the energy balance in a single polymer chain:

$$\frac{d}{dt} \int_{V_0} H(\mathbf{F}, \mathbf{E}) dV_0 - \frac{d}{dt} \int_{\mathbb{R}^3} \frac{\epsilon_0}{2} \mathbf{E} \cdot \mathbf{E} dV = \frac{dW}{dt} + T \frac{d}{dt} \int_{V_0} S(\mathbf{F}, \mathbf{E}) dV_0, \quad (9)$$

where, ~~in the current configuration~~, we consider a dielectric body that occupies the region  $V_0 \subset \mathbb{R}^3$  with a boundary  $\partial V_0$  before the deformation and the region  $V \subset \mathbb{R}^3$  with a boundary  $\partial V$  after the deformation, ~~at the current configuration~~.

The rate of ~~change in the~~ electric enthalpy is [?]

$$\frac{d}{dt} \int_{V_0} H(\mathbf{F}, \mathbf{E}) dV_0 = \int_V \frac{1}{J} \frac{\partial H(\mathbf{F}, \mathbf{E})}{\partial \mathbf{F}} \mathbf{F}^T : \mathbf{L} dV + \int_V \frac{1}{J} \frac{\partial H(\mathbf{F}, \mathbf{E})}{\partial \mathbf{E}} \cdot \dot{\mathbf{E}} dV, \quad (10)$$

and the rate of ~~change in~~ entropy is

$$\frac{d}{dt} \int_{V_0} S(\mathbf{F}, \mathbf{E}) dV_0 = \int_V \frac{1}{J} \frac{\partial S(\mathbf{F}, \mathbf{E})}{\partial \mathbf{F}} \mathbf{F}^T : \mathbf{L} dV + \int_V \frac{1}{J} \frac{\partial S(\mathbf{F}, \mathbf{E})}{\partial \mathbf{E}} \cdot \dot{\mathbf{E}} dV. \quad (11)$$

If we assume no free charges in the material and neglect body forces, the power extracted by the external mechanical and electrical agents on the system is [???

$$\frac{dW}{dt} = \int_{\partial V} \mathbf{t} \cdot \mathbf{v} dA - \int_{\partial V} \rho_a \frac{d\phi}{dt} dA, \quad (12)$$

which can also be formulated as [?]

$$\frac{dW}{dt} = \int_V (\boldsymbol{\sigma} - \boldsymbol{\sigma}^M - \mathbf{E} \otimes \mathbf{P}) : \mathbf{L} dV - \frac{d}{dt} \int_{\mathbb{R}^3} \frac{\epsilon_0}{2} \mathbf{E} \cdot \mathbf{E} dV - \int_V \mathbf{P} \cdot \dot{\mathbf{E}} dV + \int_{\mathbb{R}^3/V} (\boldsymbol{\sigma} - \boldsymbol{\sigma}^M) : \mathbf{L} dV. \quad (13)$$

By ~~takin into account~~ using Eqs. (10), ~~Eq.~~ (11), and ~~Eq.~~ (13) in Eq. (9), we obtain

$$\begin{aligned} & \int_V \left( \frac{1}{J} \left( T \frac{\partial S(\mathbf{F}, \mathbf{E})}{\partial \mathbf{E}} - \frac{\partial H(\mathbf{F}, \mathbf{E})}{\partial \mathbf{E}} \right) - \mathbf{P} \right) \cdot \dot{\mathbf{E}} dV + \int_{\mathbb{R}^3/V} (\boldsymbol{\sigma} - \boldsymbol{\sigma}^M) : \mathbf{L} dV + \\ & \int_V \left( \boldsymbol{\sigma} - \boldsymbol{\sigma}^M - \mathbf{E} \otimes \mathbf{P} - \frac{1}{J} \left( \frac{\partial H(\mathbf{F}, \mathbf{E})}{\partial \mathbf{F}} - T \frac{\partial S(\mathbf{F}, \mathbf{E})}{\partial \mathbf{F}} \right) \mathbf{F}^T \right) : \mathbf{L} dV = 0. \end{aligned} \quad (14)$$

~~As it is~~ Because we have assumed that Eq. (14) fits every acceptable process, ~~by~~ we can

Figure 1: A schematic description of the coordinate system  $\{\hat{\mathbf{E}}, \hat{\mathbf{Y}}, \hat{\mathbf{Z}}\}$  and the applied spherical coordinates.

following ? it is to obtained that

$$\boldsymbol{\sigma} = \boldsymbol{\sigma}^m + \mathbf{E} \otimes \mathbf{P} + \boldsymbol{\sigma}^M, \quad (15)$$

where

$$\boldsymbol{\sigma}^m = \frac{1}{J} \left( \frac{\partial H(\mathbf{F}, \mathbf{E})}{\partial \mathbf{F}} - T \frac{\partial S(\mathbf{F}, \mathbf{E})}{\partial \mathbf{F}} \right) \mathbf{F}^T, \quad (16)$$

is the mechanical stress [?], and  $\mathbf{E} \otimes \mathbf{P}$  is the polarization stress ~~where~~, with

$$\mathbf{P} = \frac{1}{J} \left( T \frac{\partial S(\mathbf{F}, \mathbf{E})}{\partial \mathbf{E}} - \frac{\partial H(\mathbf{F}, \mathbf{E})}{\partial \mathbf{E}} \right). \quad (17)$$

Furthermore, when dealing with incompressible materials,

$$\boldsymbol{\sigma} = \boldsymbol{\sigma}^m + \mathbf{E} \otimes \mathbf{P} + \boldsymbol{\sigma}^M + p_* \mathbf{I}, \quad (18)$$

where  $p_*$  is an arbitrary Lagrange multiplier corresponding to the indeterminate hydrostatic pressure that results from the incompressibility constraint and  $\mathbf{I}$  is the identity matrix. The corresponding deviatoric stress, which is related to shape change, is

$$\boldsymbol{\sigma}_{\text{Dev}} = \boldsymbol{\sigma} - \frac{\text{tr}(\boldsymbol{\sigma})}{3} \mathbf{I}. \quad (19)$$

## 2.2 Entropy-driven electro-elasticity of an isotropic polymer network

(Note: defining the construct and directions in the polymer)

~~According to t~~The work of ?; ~~in order to~~ indicates that ~~evaluate~~ analyzing the properties and structure of different polymers ~~the analysis~~ starts with a single polymer chain with  $n$  dipolar monomers. ~~The~~Let  $l$  be the length between the two contact points of a monomer with its neighbors ~~is l~~. ~~We~~ and define a coordinate system  $\{\hat{\mathbf{E}}, \hat{\mathbf{Y}}, \hat{\mathbf{Z}}\}$  (Fig. 1) ~~as for the~~ chain ~~is~~ subjected to an electric field  $\mathbf{E} = E\hat{\mathbf{E}}$ . In this system,

$$\hat{\boldsymbol{\xi}} = \cos \theta \hat{\mathbf{E}} + \sin \theta (\cos \phi \hat{\mathbf{Y}} + \sin \phi \hat{\mathbf{Z}}) \quad (20)$$

is a unit vector where  $0 \leq \theta < \pi$  is the angle between  $\hat{\xi}$  and the electric field and  $0 \leq \phi < 2\pi$  is the angle of its projection onto the plane perpendicular to  $\hat{\mathbf{E}}$  and  $\hat{\mathbf{Y}}$ . We define  $d\Gamma = \sin \theta d\theta d\phi$  as the differential solid angle. ~~We also formally define that and allow  $\Gamma$  to vary in the range~~ from 0 to  $\Gamma_0$ .

(**Note:** a chain's number of possible configurations and constraints (+Stirling's approximation))

The number of possible configurations of a single polymer chain is

$$\Omega^C = \frac{n!}{\prod_i (n_i!)}, \quad (21)$$

where  $n_i$  represents the number of dipolar monomers aligned along  $\hat{\xi}$  in the range  $\theta_i \leq \theta < \theta_i + d\theta$  and  $\phi_i \leq \phi < \phi_i + d\phi$ . For convenience, we define that  $\theta_i$  and  $\phi_i$  correspond to the unit vector  $\hat{\xi}_i$ . The entropy of the chain is

$$S^C = k \ln(\Omega^C) = k \left( n \ln(n) - n - \sum_i n_i \ln(n_i) + \sum_i n_i \right), \quad (22)$$

where we have used Stirling's approximation is implemented and  $k$  is Boltzmann's constant. The chain is subjected to three constraints:

$$\sum_i n_i = n, \quad (23)$$

$$\sum_i l n_i \hat{\xi}_i = \mathbf{r}, \quad (24)$$

where the end-to-end vector of the monomers chain is  $\mathbf{r} = r \hat{\mathbf{r}}$ , with  $\hat{\mathbf{r}} = \cos \Theta \hat{\mathbf{E}} + \sin \Theta (\cos \Phi \hat{\mathbf{Y}} + \sin \Phi \hat{\mathbf{Z}})$ , and

$$\sum_i n_i h_i = H^C, \quad (25)$$

where  $h_i$  is the electrical enthalpy electric enthalpy of a monomer directed along  $\hat{\xi}_i$  and  $H^C$  is the enthalpy of the chain.

(**Note:** maximizing the entropy according to the constraints)

We assume that the polymer chain occupies the most probable configuration under the given constraints, and therefore we are interested in maximizing the entropy;

$$S^C = k \left[ \ln(\Omega^C) + \alpha \left( \sum_i n_i - n \right) + \boldsymbol{\tau} \cdot \left( \sum_i n_i \hat{\xi}_i - \frac{\mathbf{r}}{l} \right) + \gamma \left( \sum_i n_i h_i - H^C \right) \right], \quad (26)$$

where  $\alpha$ ,  $\boldsymbol{\tau}$ , and  $\gamma$  are Lagrange multipliers. The derivative of  $S_C$  with respect to  $n_i$  is

$$\frac{\partial S^C}{\partial n_i} = k \left[ -\ln(n_i) + \alpha + \boldsymbol{\tau} \cdot \hat{\xi}_i + \gamma h_i \right] = 0, \quad (27)$$

from which

$$n_i = \exp\left(\alpha + \boldsymbol{\tau} \cdot \hat{\boldsymbol{\xi}}_i + \gamma h_i\right). \quad (28)$$

Upon substitution of the latter into Eq. (26), the maximum entropy that can be achieved by the chain is [?];

$$S^C = k \left[ n \ln(n) - \alpha n - \boldsymbol{\tau} \cdot \frac{\mathbf{r}}{l} - \gamma H^C \right]. \quad (29)$$

**(Note: Lagrange multiplier - inverse temperature)**

We assume that the polymer chains do not interact with one another. Consequently, in a volume element  $dV_0$ , the total entropy -density and the total electrical-enthalpy -density function are  $S = \frac{1}{dV_0} \sum_k S_k^C$  and  $H = \frac{1}{dV_0} \sum_k H_k^C$ , respectively. Applying counting for the first law of thermodynamics with respect to the enthalpy of the  $k$ -th chain, we obtain

$$\frac{\partial H}{\partial H_k^C} = T \frac{\partial S}{\partial H_k^C}, \quad (30)$$

from which we can derive the relation

$$\gamma = -\frac{1}{kT} \quad (31)$$

wherewith the help of Eq. (29) is used.

**(Note: PDF of a monomer according to the constraints and with maximum entropy (+calculating the rest of the Lagrange multipliers and Hc))**

From the constraints Eq.(23) and Eq.(27), we obtain

$$\sum_i n_i = \exp(\alpha) \int_0^{\Gamma_0} \exp\left(\boldsymbol{\tau} \cdot \hat{\boldsymbol{\xi}} - \frac{h}{kT}\right) d\Gamma = n, \quad (32)$$

where Eq. (29) is used and the summation is replaced by an integral over all the monomer orientations of the monomers. Therefore,

$$\exp(\alpha) = \frac{n}{Z}, \quad (33)$$

where

$$Z = \int_0^{\Gamma_0} \exp\left(\boldsymbol{\tau} \cdot \hat{\boldsymbol{\xi}} - \frac{h}{kT}\right) d\Gamma, \quad (34)$$

is the partition function. Subsequently, from Eq. (28) we have that

$$p(\hat{\boldsymbol{\xi}}, h) = \frac{1}{Z} \exp\left(\boldsymbol{\tau} \cdot \hat{\boldsymbol{\xi}} - \frac{h}{kT}\right) \quad (35)$$

is the probability density function (PDF) that a monomer is aligned in the direction  $\hat{\boldsymbol{\xi}}$  and

has an electrical enthalpy  $h$ . An implicit equation ~~from which~~ that gives the Lagrange multiplier  $\tau$  ~~is computed~~ follows from constraint Eq-(24):

$$\int_0^{l_0} \hat{\boldsymbol{\xi}} p \, d\Gamma = \frac{\mathbf{r}}{nl}. \quad (36)$$

From Eq. (25) the enthalpy of the chain is

$$\int_0^{l_0} h p \, d\Gamma = H^C. \quad (37)$$

(Note: monomer enthalpy and different dipole types)

Following ??? and ?, the ~~electrical enthalpy~~ electric enthalpy of a dipole oriented along  $\hat{\boldsymbol{\xi}}$  is

$$h = \mathbf{m} \cdot \mathbf{E}, \quad (38)$$

where the dipole vector  $\mathbf{m}$  is determined according to a relevant model that represents the local relation. ~~We account for~~ three specific models ~~were accounted for~~, the first of which corresponds to a spontaneous dipole or a rigid dipole with a constant magnitude [?]

$$\mathbf{m}_S = \kappa_P \hat{\boldsymbol{\xi}}. \quad (39)$$

The second model is of a uniaxial dipole whose magnitude depends on the electric field [?]:

$$\mathbf{m}_U = \kappa_U \hat{\boldsymbol{\xi}} \otimes \hat{\boldsymbol{\xi}} \mathbf{E}, \quad (40)$$

where  $\kappa_U$  is commonly referred to as the *polarizability* of the dipole. The third type is the transversely isotropic (TI) model [?]:

$$\mathbf{m}_{TI} = \frac{1}{2} \kappa_{TI} (\mathbf{I} - \hat{\boldsymbol{\xi}} \otimes \hat{\boldsymbol{\xi}}) \mathbf{E}, \quad (41)$$

where ~~in this case~~ the dipole is perpendicular to  $\hat{\boldsymbol{\xi}}$ . Note that ~~since~~ we do not account for the local electrostatic interactions between the dipolar monomers, ~~so thea~~ uniform electric field is induced over the monomers in the chain ~~is uniform~~.

~~We note that in order to have that~~ For three dielectrics composed of a random and uniform distribution of spontaneous, uniaxial, and transversely isotropic dipoles ~~admitto~~ behave the same ~~behavior~~ in the limit of infinitesimal deformations and small electric fields, ~~the relations~~ we impose  $\kappa_U = \kappa_{TI} = \frac{\kappa_P^2}{kT} = \kappa$  ~~are set~~. The polarizability is ~~taken~~ as  $\kappa = \frac{3}{n_0} \epsilon_0 \chi_0$  [?], where  $\chi_0 = \epsilon_r - 1$  is the initial susceptibility and  $\epsilon_r$  is the relative permittivity.  $n_0 = N n$  is the number of monomers in a unit referential volume where  $N$

is the number of chains in the unit referential volume.

(Note: PDF in the amorphous case)

For an amorphous polymer, the chain's constraints, presented given in by Eqs. (23), Eq-(24), and Eq-(25), are irrelevant as therebecause are no such limitations exist onfor a single monomer. Therefore,  $\tau = 0$  and the adjusted form of the PDF in Eq. (35) is

$$p(\hat{\xi}) = \frac{1}{Z} \exp\left(-\frac{h}{kT}\right), \quad (42)$$

where

$$Z = \int \exp\left(-\frac{h}{kT}\right) d\Gamma, \quad (43)$$

and the enthalpy of the monomer is calculated by using Eq. (38) according to with the correct dipole type.

(Note: analytical calculation - PDF in the amorphous case - U and TI)

In addition to the numerical calculations for the PDF in the amorphous case, the amorphous monomer distribution can also be calculated by applying the analytical analysis presented by of ?, as giving

$$p_U = \frac{\omega}{4\pi D(\omega)} \exp\left[-\omega^2 \sin^2(\theta_i)\right] \quad (44)$$

is the PDF of the uniaxial dipole, where  $\omega = \sqrt{\frac{\kappa}{kT}} E = \frac{\kappa_P E}{kT}$  and  $D(\omega) = \exp(-\omega^2) \int_0^\omega \exp(t^2) dt$  is the Dawson function. The PDF for the TI dipole is

$$p_{TI} = \frac{\omega}{(2\pi)^{3/2} \text{Erf}\left(\frac{\omega}{\sqrt{2}}\right)} \exp\left[-\frac{\omega^2}{2} \cos^2(\theta_i)\right], \quad (45)$$

where  $\text{Erf}(x)$  is the error function.

## 2.3 Phenomenological approach to electro-elasticity

(Note: A reference for the results in the application section)

We compare the results of the theory developed above with those of a relatively simple phenomenological predictive material model, a relatively simple model that allows reasonable assumptions, and is based on settings of continuum mechanics is used from the phenomenological viewpoint as a comparison to the results of our examinations. In the current work, a constitutive law for the material is required to must be expressed through an energy-density function that depends on both the deformation and the electric displacement or the electric field. Thus, as a reference, we recall the extended neo-Hookean

energy-density function for an ideal elastic dielectric (IED) [?]:

$$W(\mathbf{F}, \mathbf{E}) = \frac{\mu}{2} [\text{Tr}(\mathbf{F}^T \mathbf{F} - \mathbf{I})] + \frac{\epsilon_0 \epsilon_r}{2} \mathbf{E} \cdot \mathbf{E}, \quad (46)$$

where  $\mu$  is the shear modulus of the material. From Eq. (46) and ~~on the basis of thermodynamic arguments~~, assuming ~~a~~ conservation of energy and a reversible or conservative material, the constitutive equations for an incompressible IED can be expressed as

$$\boldsymbol{\sigma} = \mathbf{F} \frac{\partial W}{\partial \mathbf{F}} + p_* \mathbf{I} = \mu \mathbf{F} \mathbf{F}^T + \mathbf{E} \otimes \mathbf{D} + p_* \mathbf{I}, \quad (47)$$

and

$$\mathbf{D} = \epsilon_0 \epsilon_r \mathbf{E}, \quad (48)$$

in accordance with Eq. (3) ~~as with~~ the relative permittivity ~~is~~ considered to be constant. ~~We n~~Note that, in general, this model does not accurately ~~retrieves~~~~reproduce~~ experimental results for coupled electromechanical loading.

Figure 2: Schematic description of an arbitrary one dimensional system subjected to electromechanical excitation at its boundary.

### 3 Electro-elasticity of solutions and anisotropic networks of polymer molecules

We now present an in-depth multiscale analysis of the electromechanical coupling in DEs, which is based on their inherent microstructure, is carried out. This analysis allows us to examine the interplay between the macroscopic deformation of the DEs and the rearrangement of the monomers in a network of polymer chains as a result of external electrical and mechanical loading will be examined.

#### 3.1 First law of thermodynamics

The first law of thermodynamics, presented expressed in Eq. (8), is formulated as a general representation for of the electromechanical situation. Such This representation accounts for the conservation of energy of in a body that is subjected to an electric field while allowing us to formulate the energy balance in terms of the electric enthalpy and the entropy of the system.

To systematically analyze of the electromechanical coupling in polymers, from the microscopic to the macroscopic levels, we specialize tailor Eq. (8) to five different systems. The simplest ones systems are based on the system that presented in Fig. 2, which is essentially a one-dimensional system. Subsequently, we examine a network that is treated as a 3-D three-dimensional body.

#### 3.2 One-dimensional 1-D systems of charges, dipoles, and molecular chains in an electric field

In a 1-D one-dimensional system (see Fig. 2), we define the vector connecting the two ends (i.e., the end-to-end vector of the system) as  $\mathbf{r} = \mathbf{r}_- - \mathbf{r}_+$ . The quantities  $\mathbf{f}^{+/-}$ ,  $\mathbf{V}^{+/-}$ , and  $Q^{+/-}$  are the forces, velocities, and charges, respectively, on at the system's boundaries, respectively. The rate of change in enthalpy and the rate of entropy are  $\dot{H}^r = \dot{H}(\mathbf{r}, \mathbf{E}_0)$  and  $\dot{S}^r = \dot{S}(\mathbf{r}, \mathbf{E}_0)$ , respectively. The power extracted by the external agents [see (Eq. (12))] is  $\dot{W}^r = \sum \mathbf{f} \cdot \mathbf{V} + \sum Q \dot{\phi}$ .

Figure 3: Schematic description of a single charge subjected to an electric field.

### 3.2.1 A single electric charge

We begin ~~with an~~by analyzing ~~of~~ the second term ~~in~~of Eq. (8), ~~that~~which concerns the variation in the energy of the system due to variations in the electric field generated by a single charge. To be precise, the present case describes a ~~zero-dimensional~~ $\theta$ - $\mathbb{D}$  system.

The electric field due to a particle with a constant electric charge  $Q$  is derived from Coulomb's law as

$$\mathbf{E}^Q(\mathbf{g}) = \frac{Q\hat{\mathbf{g}}}{4\pi\epsilon_0g^2}, \quad (49)$$

where in the current case  $\mathbf{g} = g\hat{\mathbf{g}}$  is the vector from a specific point in space to the charge's location. Thus, ~~as~~because electric fields satisfy the superposition principle, the total electric field at the ~~mentioned~~given location is

$$\mathbf{E}(\mathbf{g}) = \mathbf{E}_0 + \mathbf{E}^Q(\mathbf{g}) = \mathbf{E}_0 + \frac{Q\hat{\mathbf{g}}}{4\pi\epsilon_0g^2}, \quad (50)$$

where  $\mathbf{E}_0 = E_0\hat{\mathbf{E}}$  is the electric field ~~subjected~~imposed on the entire space. Accordingly, the second term in Eq. (8) is

$$\begin{aligned} & \frac{\epsilon_0}{2} \frac{d}{dt} \int_{\mathbb{R}^3} \left( \mathbf{E}_0 \cdot \mathbf{E}_0 + 2 \frac{Q\mathbf{E}_0 \cdot \hat{\mathbf{g}}}{4\pi\epsilon_0g^2} + \frac{Q\hat{\mathbf{g}}}{4\pi\epsilon_0g^2} \cdot \frac{Q\hat{\mathbf{g}}}{4\pi\epsilon_0g^2} \right) dV \\ &= \frac{\epsilon_0}{2} \frac{d}{dt} \int_{\mathbb{R}^3} \left( \mathbf{E}_0 \cdot \mathbf{E}_0 + \frac{Q\mathbf{E}_0 \cdot \hat{\mathbf{g}}}{2\pi\epsilon_0g^2} + \frac{Q^2}{16\pi^2\epsilon_0^2g^4} \right) dV. \end{aligned} \quad (51)$$

~~We n~~Note that the first and third terms in Eq. (51) are constants. Moreover, for any spherical region about ~~the~~a charge with inner radius  $R_i$  and outer radius  $R_o$ , the variation in the energy depends on

$$\frac{Q}{4\pi} \int_0^{2\pi} \int_0^\pi \int_{R_i}^{R_o} \frac{\mathbf{E}_0 \cdot \hat{\mathbf{g}}}{g^2} g^2 \sin \Theta dg d\Theta d\Phi = \frac{QE_0}{2} \frac{d}{dt} \int_{R_i}^{R_o} dg \int_0^\pi \cos \Theta \sin \Theta d\Theta \equiv 0, \quad (52)$$

where ~~according to Eq. (20)~~ $\mathbf{E}_0 \cdot \hat{\mathbf{g}} = E_0 \cos \Theta$  [Eq. (20)]. Since this integral vanishes identically, so does its time derivative. Thus, for any motion of a single charge in a uniform electric field, the second term in Eq. (8) vanishes.

Taking into account Eq. (52) and neglecting the enthalpy and entropy, ~~as~~ since we assume no material, Eq. (8) is reduced to  $\dot{W} = 0$ . Thus, ~~based on~~observing Fig. 3 and

Figure 4: Schematic description of a single dipole consisting of two charges,  $Q^+$  and  $Q^-$ , connected by a stiff rod in an electric field.

from Eq. (12), we obtain for a single charge

$$\dot{W} = \mathbf{f} \cdot \frac{d\mathbf{c}}{dt} - Q \frac{d\phi}{dt} = 0, \quad (53)$$

where  $\mathbf{c}$  denotes the location of the charge. The velocity of the charge is  $\mathbf{V} = \frac{d\mathbf{c}}{dt}$  where  $d\mathbf{c} = \delta\hat{\mathbf{E}} + d\mathbf{c}_T$  represents the change in the location position of the charge during the time interval  $dt$ ,  $d\phi = -\mathbf{E}_0 \cdot d\mathbf{c} = -\delta E_0$ , and  $\mathbf{f} = f_E \hat{\mathbf{E}} + \mathbf{f}_T$ . Moreover,  $d\mathbf{c}_T$  and  $\mathbf{f}_T$  are the components of  $d\mathbf{c}$  and  $\mathbf{f}$ , respectively, that are perpendicular to the direction  $\hat{\mathbf{E}}$ . Thus,

$$\dot{W} = \frac{d}{dt} (\mathbf{f} \cdot d\mathbf{c} + Q\delta E_0) = \frac{d}{dt} (f_E \delta + \mathbf{f}_T \cdot d\mathbf{c}_T + Q\delta E_0) = 0. \quad (54)$$

Therefore, since in an equilibrium state because Eq. (54) equals zero in an equilibrium state and  $d\mathbf{c}_T$  is arbitrary, we conclude that  $\mathbf{f}_T \equiv 0$  and  $f_E = -QE_0$ . This is precisely Coulomb's force on a charge of magnitude  $Q$  in an electric field  $\mathbf{E}_0$ .

### 3.2.2 Dipoles

Consider now a charged nonpolarized rigid dipole and, as in the previous case, we assume no material and neglect the enthalpy and entropy. As can be seen indicated in Fig. 4, the dipole is described as consists of two charges,  $Q^+$  and  $Q^-$ , connected by a stiff rod of length  $l$  and oriented in the direction of the unit vector  $\hat{\boldsymbol{\xi}}$ . We assume that  $Q^+ = -Q^- = Q$ .

Again, we begin with an analysis of the second term in Eq. (8), which gives the variation in the system energy of the system due to variations in the electric field generated by both the charges. Hence Thus, in accordance with the superposition principle,

$$\begin{aligned} \mathbf{E} &= \mathbf{E}_0 + \mathbf{E}^{Q^+}(\mathbf{g}^+) - \mathbf{E}^{Q^-}(\mathbf{g}^-) = \mathbf{E}_0 + \frac{Q\hat{\mathbf{g}}^+}{4\pi\epsilon_0(g^+)^2} - \frac{Q\hat{\mathbf{g}}^-}{4\pi\epsilon_0(g^-)^2} \\ &= \mathbf{E}_0 + \mathbf{E}^+ + \mathbf{E}^-, \end{aligned} \quad (55)$$

where  $\mathbf{g}^+ = g^+\hat{\mathbf{g}}^+$  and  $\mathbf{g}^- = g^-\hat{\mathbf{g}}^-$  are the vectors from a specific point in space to the locations positions of the charges  $Q^+$  and  $Q^-$ , respectively. Accordingly, the second term

in Eq. (8) is

$$\frac{\epsilon_0}{2} \frac{d}{dt} \int_{\mathbb{R}^3} \left( \mathbf{E}_0 \cdot \mathbf{E}_0 + 2 \left( \mathbf{E}_0 \cdot \mathbf{E}^+ + \mathbf{E}_0 \cdot \mathbf{E}^- + \mathbf{E}^+ \cdot \mathbf{E}^- \right) + \mathbf{E}^+ \cdot \mathbf{E}^+ + \mathbf{E}^- \cdot \mathbf{E}^- \right) dV, \quad (56)$$

where, according to Eq. (52), the integrals ~~of~~  $\mathbf{E}_0 \cdot \mathbf{E}^+$  and  $\mathbf{E}_0 \cdot \mathbf{E}^-$  vanishes identically and the ~~rest of the remaining~~ terms are constants. Hence Thus, Eq. (56) equals zero.

Thus As a result, Eq. (8) is again reduced to  $\dot{W} = 0$ . From the definition of the electric potential,  $d\phi = -\mathbf{E}_0 \cdot d\mathbf{c}$ . Thus, so  $\dot{\phi}^{+/-} = -\mathbf{E}_0 \cdot \mathbf{V}^{+/-}$  and the rate of work of the external sources is

$$\dot{W} = \mathbf{f}^+ \cdot \mathbf{V}^+ + \mathbf{f}^- \cdot \mathbf{V}^- + \mathbf{E}_0 \cdot \left( Q^+ \mathbf{V}^+ + Q^- \mathbf{V}^- \right) = 0. \quad (57)$$

Since  $\mathbf{c}^+ = \mathbf{c}^- + l\hat{\xi}$  from the geometry ~~ie relation~~ of the situation, then  $\mathbf{V}^+ = \mathbf{V}^- + l\dot{\hat{\xi}}$  and the corresponding rate of work is

$$\dot{W} = (\mathbf{f}^+ + \mathbf{f}^-) \cdot \mathbf{V}^- + l(\mathbf{f}^+ + Q\mathbf{E}_0) \cdot \dot{\hat{\xi}} = 0. \quad (58)$$

Since Because the dipole is rigid, ~~there it is a constrained~~ along the direction of the dipole. Thus, the forces and the electric field ~~are may be splitted~~ into components in accordance with the orthogonal system  $\{\hat{\xi}, \hat{\mathbf{u}}, \hat{\mathbf{s}}\}$ , where  $\hat{\mathbf{s}} = \hat{\xi} \times \hat{\mathbf{E}}$  is perpendicular to the plane spanned by the electric field and the dipole.  $\hat{\mathbf{u}} = \hat{\mathbf{s}} \times \hat{\xi}$  is perpendicular to the dipole and is on the ~~described given~~ plane. Hence, let Using  $\mathbf{f}^+ = a^+ \hat{\xi} + b^+ \hat{\mathbf{u}} + c^+ \hat{\mathbf{s}}$ ,  $\mathbf{f}^- = a^- \hat{\xi} + b^- \hat{\mathbf{u}} + c^- \hat{\mathbf{s}}$ , and  $\mathbf{E}_0 = e\hat{\xi} + g\hat{\mathbf{u}}$ . Consequently, Eq. (58) yields

$$\dot{W} = \left[ (a^+ + a^-) \hat{\xi} + (b^+ + b^-) \hat{\mathbf{u}} + (c^+ + c^-) \hat{\mathbf{s}} \right] \cdot \mathbf{V}^- + l \left[ a^+ \hat{\xi} + b^+ \hat{\mathbf{u}} + c^+ \hat{\mathbf{s}} + Q(e\hat{\xi} + g\hat{\mathbf{u}}) \right] \cdot \dot{\hat{\xi}} = 0. \quad (59)$$

Since ~~at equilibrium~~ Eq. (59) equals zero ~~at equilibrium~~ and  $\mathbf{V}^-$  and  $\dot{\hat{\xi}}$  are arbitrary, ~~it can be inferred from~~ the first term implies that  $a^+ = -a^-$ ,  $b^+ = -b^-$ , and  $c^+ = -c^-$ . ~~Though However,~~ when consideration of ~~ing~~ the second term, ~~we can deduce~~ shows that  $c^+ = 0$ . Moreover, since  $\dot{\hat{\xi}} \perp \hat{\xi}$ , the dot product of the component ~~which is oriented~~ along the dipole with the temporal derivative of the dipole vanishes identically. Thus, the second term of Eq. (59) does not ~~contribute a constraint for~~ the components of the forces in the dipole direction and  $b^+ = -gQ$ . These results are analogous to the requirement that the sum of the ~~dipole moments on the dipole~~ vanishes.

~~In the case of~~ For a spontaneous and polarizable dipolar monomers (Fig. 5), the electrical enthalpy must be taken into account. According to ?, the ~~electrical enthalpy~~ electric enthalpy of a dipole is

$$h = -\mathbf{m} \cdot \mathbf{E}_0, \quad (60)$$

Figure 5: Schematic description of a dipole in an electric field.

where  $\mathbf{m}$  is the dipole vector. ~~In the case of~~ For a spontaneous dipole with a constant magnitude  $\kappa$ ,  $\mathbf{m} = \kappa \hat{\boldsymbol{\xi}}$ . ~~Hence~~ Thus, the ~~electrical enthalpy~~ electric enthalpy is  $h = -\kappa \hat{\boldsymbol{\xi}} \cdot \mathbf{E}_0$  and the rate of ~~the change of electrical enthalpy~~ electric enthalpy is

$$\dot{h} = -\kappa \dot{\hat{\boldsymbol{\xi}}} \cdot \mathbf{E}_0. \quad (61)$$

In this, case Eq. (8) ~~is reduced~~ to

$$\dot{h} = \dot{W}. \quad (62)$$

Substituting Eqs. (58) and ~~Eq.~~ (61) into Eq. (62) yields

$$-\kappa \dot{\hat{\boldsymbol{\xi}}} \cdot \mathbf{E}_0 = \mathbf{f}^+ \cdot \mathbf{V}^+ + \mathbf{f}^- \cdot \mathbf{V}^- = (\mathbf{f}^+ + \mathbf{f}^-) \cdot \mathbf{V}^- + l \mathbf{f}^+ \cdot \dot{\hat{\boldsymbol{\xi}}}, \quad (63)$$

which ~~yields that~~ leads to

$$(\mathbf{f}^+ + \mathbf{f}^-) \cdot \mathbf{V}^- + (l \mathbf{f}^+ + \kappa \mathbf{E}_0) \cdot \dot{\hat{\boldsymbol{\xi}}} = 0. \quad (64)$$

Again, the forces and the electric field are ~~split~~ into components in ~~accordance with~~ the orthogonal system  $\{\hat{\boldsymbol{\xi}}, \hat{\mathbf{u}}, \hat{\mathbf{s}}\}$ , where  $\mathbf{f}^+ = a^+ \hat{\boldsymbol{\xi}} + b^+ \hat{\mathbf{u}} + c^+ \hat{\mathbf{s}}$ ,  $\mathbf{f}^- = a^- \hat{\boldsymbol{\xi}} + b^- \hat{\mathbf{u}} + c^- \hat{\mathbf{s}}$ , and  $\mathbf{E}_0 = e \hat{\boldsymbol{\xi}} + g \hat{\mathbf{u}}$ . Accordingly, Eq. (58) yields

$$\left[ (a^+ + a^-) \hat{\boldsymbol{\xi}} + (b^+ + b^-) \hat{\mathbf{u}} + (c^+ + c^-) \hat{\mathbf{s}} \right] \cdot \mathbf{V}^- + \left[ l (a^+ \hat{\boldsymbol{\xi}} + b^+ \hat{\mathbf{u}} + c^+ \hat{\mathbf{s}}) + \kappa (e \hat{\boldsymbol{\xi}} + g \hat{\mathbf{u}}) \right] \cdot \dot{\hat{\boldsymbol{\xi}}} = 0. \quad (65)$$

~~Thus, as~~ Given that  $\mathbf{V}^-$  and  $\dot{\hat{\boldsymbol{\xi}}}$  are arbitrary, the first term leads ~~us~~ to the constraints  $a^+ = -a^-$ ,  $b^+ = -b^-$ , and  $c^+ = -c^-$ . The second term leads to  $c^+ = 0$  and, ~~since~~ given that  $\dot{\hat{\boldsymbol{\xi}}} \perp \hat{\boldsymbol{\xi}}$ , the second term ~~does not~~ contributes ~~anno~~ additional constraint on the components of the forces in the dipole direction and  $b^+ = -g \frac{\kappa}{l}$ . ~~In the case where~~ If  $b^+ = 0$  then  $\mathbf{E}_0 \cdot \dot{\hat{\boldsymbol{\xi}}} = 0$  for equilibrium. ~~Since and, because~~  $\dot{\hat{\boldsymbol{\xi}}} \perp \hat{\boldsymbol{\xi}}$ , ~~it inferes that for this specific case~~ we have  $\hat{\boldsymbol{\xi}} \parallel \mathbf{E}_0$  for this specific case, ~~which means that the electric field will not induce~~ causes no rotation of ~~the dipole, and so the dipole can be~~ remains at rest ~~without application~~ in the absence of external forces.

### 3.2.3 Polymer molecule (chain)

As ~~was~~ established ~~above~~, ~~while~~when  $\frac{d}{dt} \int_{\mathbb{R}^3} \mathbf{E} \cdot \mathbf{E} dV$  vanishes identically and ~~whenever~~  $\dot{W} = 0$ , Eq. (8) ~~is~~ reduces to

$$\dot{H} = T\dot{S}. \quad (66)$$

Thus, ~~since~~because  $T\dot{S}^C - \dot{H}^C = 0$  describes an equilibrium state for a polymer chain, ~~it~~ ~~means that~~ the preferred state of a chain ~~can~~may be described by determining  $\max \{TS^C - H^C\}$ . ~~By~~Then, taking Eq. (29) into account, the most probable state is the one that satisfies

$$\max \left\{ Tk \left[ n \ln(n) - \alpha n - \boldsymbol{\tau} \cdot \frac{\mathbf{r}}{l} \right] - (Tk\gamma + 1) H^C \right\}, \quad (67)$$

where ~~from~~ Eq. (25) ~~gives~~  $H^C(\mathbf{r}, \mathbf{E}_0) = \sum_{i=1}^n h_i(\hat{\boldsymbol{\xi}}_i, \mathbf{E}_0)$ . ~~Furthermore, we emphasize~~Note that the analysis ~~is executed with the~~ assumption that  $r$ , the end-to-end length of the chain with maximum permutations (i.e., the most probable length), is the only end-to-end length of chains in the direction ~~of~~  $\hat{\mathbf{r}}$ .

(Note: The "length" of a polymer chain - general)

~~In order to~~To determine the most probable length  $r$  for a specific chain, the number of possible permutations is calculated for all possible end-to-end lengths in the range  $0 \leq r \leq nl$ . This assessment is ~~performed~~done for chains in all possible orientations relative to the direction of the electric field,  $0 \leq \Theta < \pi$ . Thus, we can assess the most probable chain configuration, depending on the magnitude of the electric field in the polymerization process and the chain's inclination ~~with respect~~ to the electric field.

(Note: The "length" of a polymer chain in the case of  $\mathbf{E}=0$  - purely mechanical case)

When examining ~~the vector~~  $\mathbf{r}$  of a single polymer chain ~~in the case of~~when  $\mathbf{E}_0 = 0$ , then  $H^C(\mathbf{r}, 0) = 0$  and the entropy of the chain ~~is governing~~ its behavior. By using the implicit equation from which the Lagrange multiplier  $\boldsymbol{\tau}$  is computed and the ~~probability density function~~PDF that a monomer is in the direction  $\hat{\boldsymbol{\xi}}$ , Eqs. (36) and ~~Eq.~~ (35), respectively, we obtain

$$\frac{\int_0^{r_0} \hat{\boldsymbol{\xi}} \exp(\boldsymbol{\tau} \cdot \hat{\boldsymbol{\xi}}) d\Gamma}{\int_0^{r_0} \exp(\boldsymbol{\tau} \cdot \hat{\boldsymbol{\xi}}) d\Gamma} = \frac{\mathbf{r}}{nl}. \quad (68)$$

Let  $\boldsymbol{\tau} = a\hat{\mathbf{r}} + b\hat{\mathbf{m}}$ , where  $\hat{\mathbf{m}} = \frac{\mathbf{m}}{m}$  and  $\mathbf{m} = \boldsymbol{\tau} - (\boldsymbol{\tau} \cdot \hat{\mathbf{r}})\hat{\mathbf{r}}$  in an orthogonal system  $\{\hat{\mathbf{r}}, \hat{\mathbf{m}}, \hat{\mathbf{s}}\}$  where  $\hat{\mathbf{s}} = \hat{\mathbf{r}} \times \hat{\mathbf{m}}$ . In this system ~~take, define~~  $\hat{\boldsymbol{\xi}} = \cos\theta\hat{\mathbf{r}} + \sin\theta(\cos\phi\hat{\mathbf{m}} + \sin\phi\hat{\mathbf{s}})$ , ~~and~~ ~~subsequently~~which leads to  $\boldsymbol{\tau} \cdot \hat{\boldsymbol{\xi}} = a \cos\theta + b \sin\theta \cos\phi$ .

Multiplying Eq. (68) by  $\hat{\mathbf{m}}$  ~~we obtain~~ gives

$$\frac{1}{Z} \int_0^{\Gamma_0} (\hat{\boldsymbol{\xi}} \cdot \hat{\mathbf{m}}) \exp(\boldsymbol{\tau} \cdot \hat{\boldsymbol{\xi}}) d\Gamma = 0, \quad (69)$$

or ~~explicitly~~

$$\frac{1}{Z} \int_0^{2\pi} \int_0^\pi \exp(a \cos \theta) \exp(b \sin \theta \cos \phi) \sin \theta \cos \phi (\sin \theta d\theta d\phi) = 0. \quad (70)$$

~~We note~~ that the choice  $b = 0$  leads to

$$\frac{1}{Z} \int_0^\pi \exp(a \cos \theta) \sin^2 \theta d\theta \int_0^{2\pi} \cos \phi d\phi = 0, \quad (71)$$

~~and hence to the fulfilment of~~ which fulfills Eq. (69).

~~Next, by multiplying~~ the left-hand side of Eq. (68) by  $\hat{\mathbf{r}}$  ~~we obtain~~ gives

$$\frac{1}{Z} \int_0^{\Gamma_0} (\hat{\boldsymbol{\xi}} \cdot \hat{\mathbf{r}}) \exp(\boldsymbol{\tau} \cdot \hat{\boldsymbol{\xi}}) d\Gamma = \frac{1}{Z} \int_0^{2\pi} \int_0^\pi \exp(a \cos \theta) \cos \theta \sin \theta d\theta d\phi. \quad (72)$$

A change of variables to  $x = \cos \theta$  leads to ~~the expression~~

$$\frac{\int_{-1}^1 \exp(ax) x dx}{\int_{-1}^1 \exp(ax) dx} = \frac{r}{nl}, \quad (73)$$

which can be integrated to ~~obtain~~

$$\frac{\exp(a) + \exp(-a)}{\exp(a) - \exp(-a)} - \frac{1}{a} \equiv \mathcal{L}(a) = \frac{r}{nl}, \quad (74)$$

where  $\mathcal{L}$  is the Langevin function. Accordingly,

$$a = \mathcal{L}^{-1} \left( \frac{r}{nl} \right), \quad (75)$$

where  $\mathcal{L}^{-1}$  is the inverse Langevin function. Note that if  $\frac{r}{nl} \ll 1$  then  $a \cong \frac{3r}{nl}$  and  $a \rightarrow \infty$  in the limit  $r \rightarrow nl$  ~~then  $a \rightarrow \infty$ .~~

Substituting the expression for  $S^C$  following Eqs. (22) and ~~Eq.~~ (26) gives

$$\begin{aligned}\ln(\Omega^C) &= n \ln(n) - \sum_i n_i \ln(n_i) \\ &= n \left\{ \ln(n) - \frac{1}{Z} \left[ \ln\left(\frac{n}{Z}\right) \int_0^{r_0} \exp(a \cos \theta) d\Gamma + a \int_0^{r_0} \exp(a \cos \theta) \cos \theta d\Gamma \right] \right\},\end{aligned}\quad (76)$$

where, from Eq. (72),

$$\int_0^{r_0} \exp(a \cos \theta) \cos \theta d\Gamma = \frac{r}{nl} \int_0^{r_0} \exp(a \cos \theta) d\Gamma, \quad (77)$$

~~and thus, so~~

$$\begin{aligned}\ln(\Omega^C) &= n \left\{ \ln(n) - \frac{1}{Z} \left[ \left( \ln\left(\frac{n}{Z}\right) + \frac{ar}{nl} \right) \int_0^{r_0} \exp(a \cos \theta) d\Gamma \right] \right\} \\ &= n \ln(Z) - a \frac{r}{l}.\end{aligned}\quad (78)$$

~~We n~~Note that

$$Z = \frac{2\pi}{a} [\exp(a) - \exp(-a)], \quad (79)$$

~~and hence so~~

$$\ln(\Omega^C) = n \ln \left\{ \frac{2\pi}{a} [\exp(a) - \exp(-a)] \right\} - a \frac{r}{l}. \quad (80)$$

Note also that, in the limit  $r \rightarrow 0$ ,  $\ln(\Omega^S) = n \ln(4\pi)$  ~~and hence so~~  $\Omega^S = (4\pi)^n$ ; and, in the limit  $r \rightarrow nl$ ,  $\ln(\Omega^{nl}) = n \ln \left[ \frac{2\pi}{a} \exp(a) \right] - an = n \ln \left( \frac{2\pi}{a} \right)$  ~~and hence so~~  $\Omega^{nl} = \left( \frac{2\pi}{a} \right)^n \rightarrow 0$  since  $a \rightarrow \infty$ . ~~Given that  $\mathbf{E}_0 = 0$ ,  $\mathbb{T}$~~  the total number of permutations of chains with end-to-end length  $r$ , ~~as  $\mathbf{E}_0 = 0$ ,~~ is

$$\Omega^O(r) = 4\pi r^2 \Omega^C(r) = 4\pi n^2 l^2 \eta^2 \Omega^C, \quad (81)$$

where  $\eta \equiv \frac{r}{nl}$ . ~~Since at~~ In the limit  $r \rightarrow 0$ ,  $\Omega^S$  is finite ~~then~~ and  $\Omega^O(0) \rightarrow 0$ , and ~~since at~~ in the limit  $r \rightarrow nl$ ,  $\Omega^S \rightarrow 0$  and  $r^2$  is finite, so  $\Omega^O(nl) \rightarrow 0$ . This suggests that, in the range  $0 < r < nl$ ,  $\Omega^O$  has a maximum.

~~Determination of  $\mathbb{T}$~~  The maximum of  $\Omega^O$  is ~~performed as~~ obtained by using

$$\frac{d \ln \Omega^C}{d\eta} = \frac{\partial \ln \Omega^C}{\partial a} \frac{da}{d\eta} + \frac{\partial \ln \Omega^C}{\partial \eta}, \quad (82)$$

~~when~~ where we treating  $a$  and  $\eta$  as independent variables. ~~It can be seen from Eq.~~ Equations (74)

and Eq. (80) show that

$$\begin{aligned}\frac{\partial \ln \Omega^C}{\partial a} &= n \left( \frac{\exp(a) + \exp(-a)}{\exp(a) - \exp(-a)} - \frac{1}{a} \right) - \frac{r}{l} \\ &= n \left( \frac{\exp(a) + \exp(-a)}{\exp(a) - \exp(-a)} - \frac{1}{a} \right) - n\eta = 0,\end{aligned}\quad (83)$$

thusso,

$$\frac{d \ln \Omega^C}{d\eta} = -an. \quad (84)$$

From the distribution infor the case of  $\mathbf{E}_0 = 0$  [(seen in Eq. (81))]; and using as  $4\pi n^2 l^2 = k$ , we obtain

$$\frac{1}{k} \frac{\partial \Omega^O}{\partial \eta} = 2\eta \Omega^C + \eta^2 \frac{d\Omega^C}{d\eta} = \eta \exp(\ln \Omega^C) [2 - \eta a n] = 0. \quad (85)$$

Thereforeom  $a = \frac{2}{n\eta}$  or  $\eta = \mathcal{L}\left(\frac{2}{n\eta}\right) = \coth\left(\frac{2}{n\eta}\right) - \frac{n\eta}{2}$ . Ifor large  $n$  is a large number,  $\coth\left(\frac{2}{n\eta}\right) = \frac{n\eta}{2} + \frac{2}{3n\eta} + o\left(\frac{2}{n\eta}\right)^3$ . HenceThus, up to a second order in  $\frac{1}{n}$ ,  $\eta = \sqrt{\frac{2}{3}} \frac{1}{\sqrt{n}} \sim \frac{0.816}{\sqrt{n}}$ . This result differs from the assessment givenobtained from random walk statistics presented and used by ??? and ? but coincideis consistent with the assessed end-to-end chain length determined inby ? , ? , and ?.

(Note: force in a single chain with no electric field)

Furthermore, assuming zero electric field, we examine the most probable end-to-end length of a chain subjected to a force  $\mathbf{f} \parallel \mathbf{r}$  and whosewith one end is at the origin and the other end is located within a small volume  $dV = r^2 dr d\phi d\theta$  when a given force  $\mathbf{f} \parallel \mathbf{r}$  is acting upon it is also examined in the case of no electric field. By specializing Eq. (8) to the case ofFor a single chain without an no electric field, we receiveEq. (8) takes the form

$$\dot{W} + T \dot{S}^O(\mathbf{r}) = 0. \quad (86)$$

For this case, we define that  $\mathbf{r} = \rho \mathbf{R}$ , where  $\rho$  is the stretch magnitude,  $\mathbf{R}$  is the end-to-end vector in the referential state of the chain, and it iswe assumed that  $\mathbf{r} \parallel \mathbf{R}$ . Thus, in accordance with Eqs. (22) and Eq. (81), the rate of change of entropy is

$$\dot{S}^O(\mathbf{r}) = \frac{dS^O}{d\rho} \dot{\rho} = k \left( \frac{2}{\rho} - \frac{\tau \cdot \mathbf{R}}{l} \right) \dot{\rho}, \quad (87)$$

and the rate of work ofdone by the external sources is

$$\dot{W} = \mathbf{f} \cdot \mathbf{v} = \mathbf{f} \cdot \mathbf{R} \dot{\rho}, \quad (88)$$

where  $\mathbf{v} = \dot{\mathbf{r}}$ ,  $\mathbf{f}$  is the external force operatingexerted on the chain, and body forces are

neglected. Substituting Eqs. (87) and (88) into Eq. (86) yields

$$\begin{aligned} \left[ \mathbf{f} \cdot \mathbf{R} + T k \left( \frac{2}{\rho} - \frac{\tau \cdot \mathbf{R}}{l} \right) \right] \dot{\rho} &= \left[ \mathbf{f} \cdot \mathbf{R} \rho + T k \left( 2 - \frac{\tau \cdot \mathbf{R} \rho}{l} \right) \right] \dot{\rho} \\ &= [\mathbf{f} \cdot \mathbf{r} + T k (2 - \eta \tau n)] \dot{\rho} = 0, \end{aligned} \quad (89)$$

thus,

$$\mathbf{f} = -\frac{T k (2 - \eta \tau n)}{r^2} \mathbf{r} = -\frac{T k \left[ 2 - \frac{r}{nl} \mathcal{L}^{-1} \left( \frac{r}{nl} \right) n \right]}{r} \hat{\mathbf{r}}, \quad (90)$$

where Eq. (75) is taken into account. Hence, in accordance with Eq. (85), when  $\frac{r}{nl} = \sqrt{\frac{2}{3}} \frac{1}{\sqrt{n}}$  then  $\mathbf{f} = 0$ .

### 3.3 Polymer molecules (chains) in electric field

We now examine a method for controlling the electro-elastic moduli of a network. Specifically, we examine the consequence of executing the polymerization process under an external electric field. Toward this end, we assume that the polymer chains are in a solution during the polymerization. The current step assumes and that the monomers are already bonded into chains, but before that the chains are not cured and the toughened or hardened into a network of the network by cross-linking of the chains. In this case, we can refer to the chains as "floating" in the solution such that no external work is applied at their ends. Furthermore, we assume no interactions between the chains and determine their most probable permutations separately.

In accordance with the mentioned Given these assumptions, each chain will be examined individually as a. The end-to-end length of a chain is  $r_j = r(\Theta_j, \mathbf{E}_0)$  and the end-to-end direction of the chain is  $\hat{\mathbf{r}}_j = \hat{\mathbf{r}}(\Theta_j, \Phi_j)$ . According to In the coordinate system shown in Fig. 1,  $\Theta_j$  is the inclination of the chains' end-to-end vector relative to the direction of the electric field. Hence, as described in section 3.2.3, the suitable  $r_j$  for each  $\Theta_j$  is the one that satisfies Eq. (67). In the case where When  $E = 0$ , it is sufficient to analyze only a single chain need be analyzed (as detailed in section Sec. 3.2.3) since because in this case the polymer has no preferred direction in this case and the network is isotropic.

#### 3.3.1 Monomers orientational d Distribution of monomer orientation

(Note: calculating monomer orientations)

After calculating the polymers end-to-end chain length in each group, we evaluate the orientation of the chains building blocks; (i.e., the monomers, can be evaluated). The

monomer orientations are investigated as a part of a chain while taking into account the suitable constraints, as indicated by ~~seen in~~ Eqs. (23), ~~Eq. (24) and Eq. (25)~~.

Once the end-to-end chains lengths ~~with are~~ determined for the maximum possible permutations ~~are determined~~, (i.e., the most probable end-to-end chain length for each group ~~is found~~), the monomers distribution ~~can be~~ calculated for each chain by using Eq. (35). The probabilities for all possible monomer orientations ~~of the monomers~~ are then calculated ~~in order~~ to determine the monomers distribution ~~of in~~ the most probable chains, which was obtained ~~found~~ in the previous section. These ~~mentioned~~ orientations include all combinations ~~of in the ranges~~  $0 \leq \theta < \pi$  and  $0 \leq \phi < 2\pi$ .

After obtaining the monomers orientations for each ~~of the~~ chain groups, ~~we~~ comparison ~~can be made to~~ it with the monomer distribution in the amorphous ~~ease~~ phase. ~~Such distribution, which~~ can be calculated ~~according to~~ by using Eq. (42) ~~while~~ and taking into account the correct type of dipole. Analytical approximations of the PDF in the amorphous phase are ~~presented~~ given by ~~in~~ Eqs. (44) and ~~Eq. (45)~~ for uniaxial dipoles and transversely isotropic dipoles, respectively [?].

### 3.4 An anisotropic network of polymer molecules

According to ?, the total number of internal configurations of a polymer with  $N$  polymer chains is

$$\Omega^t = N! \prod_q \left( \frac{(\omega_q)^{N_q}}{N_q!} \right), \quad (91)$$

where  $\omega_q$  and  $N_q$  are the number of configurations and the number of chains associated with a specific end-to-end vector, respectively. As an example, assume, ~~in a way of an example~~, that we can *a priori* split the chains population into two populations such that, for all the end-to-end vectors in the two groups, the numbers of possible configurations are  $\omega_1$  and  $\omega_2$ ; and the numbers of chains in each group are  $N_1$  and  $N_2$ , respectively. There ~~are~~ total end-to-end vectors  $\psi_1$  and  $\psi_2$  ~~end-to-end vectors~~ in the two groups ~~such that~~ satisfy  $\psi_1 N_1 + \psi_2 N_2 = N$ . Accordingly,

$$\Omega^t = N! \left( \prod_{q_1=1}^{\psi_1} \frac{(\omega_1)^{N_1}}{N_1!} \right) \left( \prod_{q_2=1}^{\psi_2} \frac{(\omega_2)^{N_2}}{N_2!} \right) = N! \left( \frac{(\omega_1)^{N_1}}{N_1!} \right)^{\psi_1} \left( \frac{(\omega_2)^{N_2}}{N_2!} \right)^{\psi_2}. \quad (92)$$

Similarly, ~~if there are~~ given  $J$  groups with a similar number of configurations and number of chains in each group,

$$\Omega^t = N! \prod_{j=1}^J \left( \frac{(\omega_j)^{N_j}}{N_j!} \right)^{\psi_j}, \quad (93)$$

where  $\psi_j$  is the number of end-to-end vectors in ~~the~~group  $j$ -~~th~~ group and

$$\sum_j \psi_j N_j = N. \quad (94)$$

The number of possible configurations of a polymer chain is ~~calculated as~~

$$\omega_j = \frac{n_j!}{\prod_i (n_{ij}!)}, \quad (95)$$

where  $n_j$  is the number of dipolar monomers in a chain ~~which is~~ in ~~group~~the  $j$ -~~th~~ group ~~of chains~~ and  $n_{ij}$  is the number of monomers aligned ~~alongwith~~  $\hat{\xi}_i$  in a chain ~~which is~~ in ~~the~~group  $j$ -~~th~~ group. Consequently, ~~by using the Stirling approximation~~, the total entropy of the polymer is-

$$\begin{aligned} S^t &= k \ln (\Omega^t) \\ &= k \left( N \ln (N) - N + \sum_j \psi_j \left\{ N_j \left[ n_j \ln (n_j) - n_j - \sum_i n_{ij} \ln (n_{ij}) + \sum_i n_{ij} \right] - N_j \ln (N_j) + N_j \right\} \right) \\ &= k \left\{ N \ln (N) + \sum_j \psi_j N_j \left[ n_j \ln (n_j) - \sum_i n_{ij} \ln (n_{ij}) - \ln (N_j) \right] \right\}. \end{aligned} \quad (96)$$

~~by employing the Stirling approximation~~. The polymer network is subjected to the constraint mentioned in Eq. (94). As ~~was~~ previously specified, each chain is subjected to three constraints:

$$\sum_i n_{ij} = n_j, \quad (97)$$

$$\sum_i l n_{ij} \hat{\xi}_i = \mathbf{r}_j, \quad (98)$$

and the end-to-end vector of the monomers chain is  $\mathbf{r}_j = r_j \hat{\mathbf{r}}_j$ , ~~and~~so

$$\sum_i n_{ij} h_i = H_j^C, \quad (99)$$

where  $H_j^C$  is the electric ~~al~~enthalpy of the chain and  $h_i$  is the enthalpy of a monomer aligned along  $\hat{\xi}_i$ .

We assume that the most probable configuration is the ~~one~~configuration ~~that~~currently occupied by the polymer ~~occupies~~, ~~and thus~~so we are interested in maximizing the entropy

under the given constraints:

$$S^t = k \ln(\Omega_t) + k \sum_j \psi_j N_j \left[ \alpha_j \left( \sum_i n_{ij} - n_j \right) + \boldsymbol{\tau}_j \cdot \left( \sum_i n_{ij} \hat{\boldsymbol{\xi}}_i - \frac{\mathbf{r}_j}{l} \right) + \gamma_j \left( \sum_i n_{ij} h_i - H_j^C \right) \right] + k \eta \left( \sum_j \psi_j N_j - N \right), \quad (100)$$

where  $\alpha_j$ ,  $\boldsymbol{\tau}_j$ ,  $\gamma_j$ , and  $\eta$  are Lagrange multipliers.

In order to account for the maximal number of configurations, we impose that

$$\frac{\partial S^t}{\partial n_{ij}} = k \left[ -\psi_j N_j \ln(n_{ij}) + \psi_j N_j \left( \alpha_j + \boldsymbol{\tau}_j \cdot \hat{\boldsymbol{\xi}}_i + \gamma_j h_i \right) \right] = 0, \quad (101)$$

from which we obtain

$$n_{ij} = \exp \left( \frac{\psi_j N_j \left( \alpha_j + \boldsymbol{\tau}_j \cdot \hat{\boldsymbol{\xi}}_i + \gamma_j h_i \right)}{\psi_j N_j} \right) = \exp \left( \alpha_j + \boldsymbol{\tau}_j \cdot \hat{\boldsymbol{\xi}}_i + \gamma_j h_i \right). \quad (102)$$

By substituting Eq. (101) into Eq. (100), the maximum entropy of the polymer is

$$S^t = k N \ln(N) + k \sum_j \psi_j \{ N_j [n_j \ln(n_j)] - N_j \ln(N_j) \} - \sum_j \psi_j N_j \left( \alpha_j n_j + \boldsymbol{\tau}_j \cdot \frac{\mathbf{r}_j}{l} + \gamma_j H_j^C \right) + k \eta \left( \sum_j \psi_j N_j - N \right). \quad (103)$$

Following the works of ? and ?, we also assume no interaction between the polymer chains do not interact with one another. Therefore, the total enthalpy is  $H_t = \sum_j \psi_j N_j H_j^C$ . Differentiating the first law of thermodynamics [Eq. (8)] with respect to the enthalpy of the  $j$ th we have that

$$\frac{\partial H^t}{\partial H_j^C} = T \frac{\partial S^t}{\partial H_j^C}, \quad (104)$$

and by using Eq. (103), we derive the relation obtain

$$\gamma_j = -\frac{1}{kT}. \quad (105)$$

By taking into consideration the constraint imposed by Eq. (97) and the relations we received ingiven by Eqs. (102) and (105), we obtain that

$$\sum_i n_{ij} = \int_0^{\Gamma_0} \exp \left( \alpha_j + \boldsymbol{\tau}_j \cdot \hat{\boldsymbol{\xi}}_i - \frac{h_i}{kT} \right) d\Gamma = n_j. \quad (106)$$

From here we can determine the PDF, which indicates that a monomer in chain the  $j$ -th

chain is ~~in the direction of~~ oriented along  $\hat{\xi}_i$  and has an electric ~~al~~ enthalpy  $h_i$ . This is

$$p_{ij}(\hat{\xi}_i, h_i) = \frac{n_{ij}}{n_j} = \frac{1}{Z_j} \exp\left(\tau_j \cdot \hat{\xi}_i - \frac{h_i}{kT}\right), \quad (107)$$

where

$$Z_j = \int_0^{\Gamma_0} \exp\left(\tau_j \cdot \hat{\xi}_i - \frac{h_i}{kT}\right) d\Gamma, \quad (108)$$

is the partition function and the Lagrange multipliers  $\tau_j$  are computed from the implicit equations that follow from the constraints ~~in~~ given by Eq. (98),

$$\int_0^{\Gamma_0} \hat{\xi}_i p_{ij} d\Gamma = \frac{\mathbf{r}_j}{n_j l}. \quad (109)$$

The enthalpy of the chain,

$$\int_0^{\Gamma_0} h_i p_{ij} d\Gamma = H_j^C, \quad (110)$$

is computed from constraint ~~given~~ by Eq. (99).

~~In order to~~ To consider the network with ~~the~~ largest number of chain configurations, we impose that

$$\begin{aligned} \frac{\partial S^t}{\partial N_j} &= \psi_j \left[ n_j \ln(n_j) - \sum_i n_{ij} \ln(n_{ij}) - \ln(N_j) \right] + \psi_j \alpha_j \left( \sum_i n_{ij} - n_j \right) + \psi_j \tau_j \cdot \left( \sum_i n_{ij} \hat{\xi}_i - \frac{\mathbf{r}_j}{l} \right) \\ &\quad + \psi_j \gamma_j \left( \sum_i n_{ij} h_i - H_j^C \right) + \eta \psi_j \\ &= \psi_j \left[ n_j \ln(n_j) - \sum_i n_{ij} \ln(n_{ij}) - \ln(N_j) + \eta \right] = 0, \end{aligned} \quad (111)$$

from which ~~we~~ obtain

$$N_j = \exp \left[ n_j \ln(n_j) - \sum_i n_{ij} \ln(n_{ij}) + \eta \right] = \frac{\exp(\eta) n_j^{n_j}}{\prod_i n_{ij}^{n_{ij}}}. \quad (112)$$

Next, from ~~the~~ constraint ~~given~~ by Eq. (94), we obtained ~~that~~

$$\sum_j \psi_j N_j = \sum_j \psi_j \frac{\exp(\eta) n_j^{n_j}}{\prod_i n_{ij}^{n_{ij}}} = N. \quad (113)$$

This enables us to determine the Lagrange multiplier

$$\eta = \ln \left( \frac{N}{\sum_j \left( \frac{\psi_j n_j^{n_j}}{\prod_i n_{ij}^{n_{ij}}} \right)} \right). \quad (114)$$

Furthermore, the PDF that a chain is in the  $j$ -th inclination is

$$p_j = \frac{N_j}{N} = \frac{\prod_i n_{ij}^{-n_{ij}}}{\sum_k \psi_k \prod_i n_{ik}^{-n_{ik}}} = \frac{\prod_i (n_j p_{ij})^{-n_j p_{ij}}}{\sum_k \psi_k \prod_i (n_k p_{ik})^{-n_k p_{ik}}}, \quad (115)$$

and the fraction of all the chains with a specific inclination to the electric field can be estimated as

$$v_j = \psi_j p_j, \quad (116)$$

such that  $\sum_j v_j = 1$ .

Next, we ~~make~~ use of Eq. (115) in Eq. (103) to determine the entropy of the entire network:

$$\begin{aligned} S^t &= k \left\{ N \ln(N) + \sum_j \psi_j N_j \left[ n_j \ln(n_j) - \sum_i n_{ij} \ln(n_{ij}) - \ln \left( N \frac{\prod_i n_{ij}^{-n_{ij}}}{\sum_k \psi_k \prod_i n_{ik}^{-n_{ik}}} \right) \right] \right\} \\ &= k N \ln(N) + k \sum_j \psi_j N_j \left[ n_j \ln(n_j) - \sum_i n_{ij} \ln(n_{ij}) - \ln(N) \right] \\ &+ k \sum_j \psi_j N_j \left[ \sum_i n_{ij} \ln(n_{ij}) + \ln \left( \sum_k \psi_k \prod_i n_{ik}^{-n_{ik}} \right) \right] \\ &= k \left\{ \sum_j \psi_j N_j \left[ n_j \ln(n_j) + \ln \left( \sum_k \psi_k \prod_i n_{ik}^{-n_{ik}} \right) \right] \right\}. \end{aligned} \quad (117)$$

Assuming ~~that the~~ fixed number of dipolar monomers in each chain ~~is fixed~~, we neglect the first term in the last ~~line~~ of Eq. (117) to conclude that

$$S^t \propto N \ln \left( \sum_k \psi_k \prod_i n_{ik}^{-n_{ik}} \right). \quad (118)$$

By following the same steps for the case of the entropy of a chain presented in Eq. (22), ~~it can be~~ concluded that

$$S_j^C \propto \ln \left( \prod_i n_{ij}^{-n_{ij}} \right). \quad (119)$$

~~We can observe the s~~Similarities appear between both assessments of the maximum entropy. In Eq. (119), the entropy of a chain is a function of the end-to-end ~~length~~  $r_j$  and does not depend on the inclination  $\hat{r}$ .

~~We~~ Note that, ~~in the case of~~ excitation by an electric field, the number of end-

to-end vectors in ~~the group~~  $j$ -~~th group~~ are dependent on the group's inclinations with respect to the direction of the electric field, and so

$$\psi_j = 2\pi r_j^2 \sin(\Theta_j). \quad (120)$$

### 3.4.1 Deriving the properties of the polymer

~~In order to~~ To assess our methodology, we ~~wish to~~ evaluate the properties of ~~the~~ a new anisotropic polymer and to compare them ~~to~~ with those of ~~the~~ an isotropic polymer. Besides the electro-mechanical coupling, which is our main interest, the response of the polymer to purely mechanical loading and electrostatic excitation ~~should~~ is also be examined ~~too~~. The mechanical properties of the polymer relate to the mechanical stress in the polymer under purely mechanical loading described by the deformation gradient tensor  $\mathbf{F}$ . The electrical properties of the polymer, such as the electric displacement and ~~the~~ susceptibility, relate to the polarization ~~in~~ of the polymer under electrostatic excitation.

(Note: referenced mechanical stress)

The general mechanical stress presented by ?, which results from Eq. (16), is

$$\boldsymbol{\sigma}^m = \frac{1}{J dV_0} \sum_i \left[ n \left( \int_0^{r_0} \frac{\partial h}{\partial \mathbf{F}} p d\Gamma \right)_i + \frac{kT \boldsymbol{\tau}_i}{l} \frac{\partial \mathbf{r}_i}{\partial \mathbf{F}} \right] \mathbf{F}^T. \quad (121)$$

The mechanical stress takes into account the change in the electrical energy of ~~a~~ the monomers due to the mechanical deformation and ~~for~~ the mechanical loadings that deforms the ~~chains~~ end-to-end vectors of the chains. ~~Considering the assumption made by~~ As per ?, we assume that the monomer is rigid compared ~~to~~ with the polymer chain, so the ~~electrical enthalpy~~ electric enthalpy of the monomer does not depend on the deformation gradient. Furthermore, by assuming an incompressible material, Eq. (121) ~~can be~~ simplifies ~~d~~ to

$$\boldsymbol{\sigma}^m = \frac{1}{dV_0} \sum_i \left( \frac{kT \boldsymbol{\tau}_i}{l} \frac{\partial \mathbf{r}_i}{\partial \mathbf{F}} \right) \mathbf{F}^T. \quad (122)$$

(Note: simplified mechanical stress, suitable for an anisotropic case)

~~In order to~~ To ~~evaluated~~ determine the mechanical stress in the polymer, we first calculate the average stress of each chain group ~~is calculated first~~. As ~~already~~ mentioned, ~~in the case~~ ~~of~~ for excitation by an electric field, the chains groups are determined by their inclinations with respect to the ~~direction of the~~ electric field. Thus, the stresses of chains with the

same inclination,  $\Theta_k$  are averaged over  $0 \leq \Phi_q < 2\pi$  to obtain

$$\boldsymbol{\sigma}_k^m = \frac{\sum_q^Q \left( \frac{kT \tau_{kq}}{l} \frac{\partial \mathbf{r}_{kq}}{\partial \mathbf{F}} \right) \mathbf{F}^T}{Q}, \quad (123)$$

where  $\hat{\mathbf{r}}_{kq} = \cos \Theta_k \hat{\mathbf{E}} + \sin \Theta_k (\cos \Phi_q \hat{\mathbf{Y}} + \sin \Phi_q \hat{\mathbf{Z}})$ , and  $q = 1, 2, \dots, Q$ . The calculation of  $\frac{\partial \mathbf{r}_{kq}}{\partial \mathbf{F}}$  is detailed in Appendix B.

Next, we consider the relative influence of each of the chains groups is considered. This is performed by taking into account the fraction of the chains in a specific group, as shown in Eq. (116). Thus, Eq. (122) can be rewritten as

$$\boldsymbol{\sigma}^m = N \sum_k v_k \boldsymbol{\sigma}_k^m, \quad (124)$$

where the averaged stress of a chain is multiplied by the number  $N$  of chains in a unit volume,  $N$ .

(Note: referenced polarization)

The polarization

$$\mathbf{P} = -\frac{1}{J dV_0} \sum_i \left[ n \left( \int_0^{\Gamma_0} \frac{\partial h}{\partial \mathbf{E}} p d\Gamma \right)_i + \frac{kT \tau_i}{l} \frac{\partial \mathbf{r}_i}{\partial \mathbf{E}} \right], \quad (125)$$

was presented derived by ?.—This relations and stems from Eq. (17). The polarization equation, Eq. (125), considers the variation of the electrical enthalpies of the monomers as a result of the excitation of by the electric field and the reorientation of the chains as a response to the electrical excitation. From the assumption that the chains undergo affine deformation, it follows that the electric field does not directly affect the chain distribution of the chains. Thus, by assuming an incompressible material, Eq. (125) can be simplified to

$$\mathbf{P} = -\frac{n}{dV_0} \sum_i \left( \int_0^{\Gamma_0} \frac{\partial h}{\partial \mathbf{E}} p d\Gamma \right)_i. \quad (126)$$

(Note: simplified polarization, suitable for an anisotropic case + susceptibility)

The polarization of the polymer is calculated by executing the same steps that were described in the same way as for the mechanical stress. As Because  $\frac{\partial h}{\partial \mathbf{E}} = -\mathbf{m}$ , the polarizations of chains with the same of a given inclination,  $\Theta_k$  are averaged over  $0 \leq \Phi_q < 2\pi$  to obtain

$$\mathbf{P}_k = \frac{n \sum_q^Q \left( \int_0^{\Gamma_0} \mathbf{m} p d\Gamma \right)_{kq}}{Q}, \quad (127)$$

where  $q = 1, 2, \dots, Q$ .

Thus, ~~as~~because the relative influence of each ~~of the~~chains groups is considered through the fraction of ~~the~~chains in a specific group, ~~we~~ obtain

$$\mathbf{P} = N \sum_k v_k \mathbf{P}_k, \quad (128)$$

where the averaged polarization of a chain is multiplied by the number  $N$  of chains ~~in~~ ~~aper~~ unit volume,  ~~$N$~~ . After ~~the~~ calculationg ~~of~~ the polarization, the electric displacement ~~may~~can be calculated ~~according to~~by using Eq. (3), and the susceptibility can be calculated ~~by using~~as

$$\chi = \frac{\mathbf{P} \cdot \mathbf{E}}{\epsilon_0 E^2}. \quad (129)$$

## 4 Application to electrostatically biased network

(Note: Opening sentence + Isotropic example - first step of the numerical analysis - evaluating the Lagrange multiplier  $\tau$ )

To modify the DE properties of DEs in order to affect modify their the electromechanical coupling of polymers, we propose to perform the polymerization process of a polymer monomers while in the presence of an external electric field. Such a process will result in produces a relative order of the polymer-chain networks of polymer chains as the chains and the dipolar monomers can react to the electric field while the chains are forming and "floating" in the solution state. The mentioned electric field will be removed at the end of after the polymer-chain network hardens ing of the network which is a result of the cross-linking between of the chains. We note that the chain and monomer responses of the chains and monomers are are restricted by the constraints in Eq. (94) and, Eq. (97), Eq. (98) and Eq. (99), as is detailed in section Sec. 3.4.

To examine the influence of our the proposed polymerization process (i.e., creating a "biased" polymer), we follow the analytical analysis detailed in section Sec. 3. This examination will be executed is done while comparing the our results for the biased polymer with to those of an unbiased polymer (i.e., an isotropic polymer) and with to the IED model (presented in section Sec. 2.3), all in order to evaluate the influence of performing how the suggested process affects on the structure and properties of the polymer.

### 4.1 Chains distribution

The initial step of the analysis is to evaluate determine the most probable configurations of the polymer chains in of the isotropic and biased polymers. At first w We first apply our calculations to the case of no electric field, and for a network of n isotropic chain networks. The initial step of the calculation is to evaluate determine the value of the Lagrange multiplier  $\tau$  with the by application of using the Newton-Raphson method onto Eq. (36). The first guess,  $\tau_0$ , is obtained by analytically estimating the Lagrange multiplier as a function of  $\mathbf{r}$  in a case where the electric field approaches zero,

$$\tau_0 = \frac{3\mathbf{r}}{nl}, \quad (130)$$

which is accurate in this specific case, as is detailed in Appendix C.

(Note: chains length - isotropic distribution)

As a result of Given the maximum-entropy assumption and the fact that, in this case, there is no electric actuation or any other external influence, we can assume that there

is an isotropic distribution of chains, which means that and so we can assess the end-to-end length of a chain in a single direction and relate it to all directions. Thus, in order to determine/evaluate the most probable end-to-end chain length, the number of configurations of a chain with a specific  $\mathbf{r}$  is calculated and then multiplied by the surface area of a sphere with the same  $r$ , which represents the chains groups in the isotropic case, as is discussed in section Sec. 3.2.3 and shown in by Eq. (81). The entropy for each case is calculated by using the results from of Eq. (81) in Eq. (22). An Several examples are is presented in Fig. 6, which presents/shows the entropy as a function of the normalized radius,  $\frac{r}{nl}$ , for  $n = 50$  and  $n = 100$  with  $l = 100 \mu\text{m}$ . The initial susceptibility used in these presented examples is  $\chi_0 = 37$ , which is about ten times the electric susceptibility of the commercially available polymer VHB 4910, and. The analyses are performed/done for the case of uniaxial dipoles. The difference between the curves in Fig. 6 can be attributed to Eqs. (21), Eq-(22), and Eq-(81). Accordingly, the entropy of the chain increases with as the number of monomers in the chain increases so does the entropy of the chain.

(Note: defining calculation parameters - material properties and calculations boundaries)

We assume that the shear modulus  $\mu = 10^5 \text{ Pa}$  for the polymer in its initial unloaded configuration. is  $\mu = 10^5 \text{ Pa}$ . The value of  $N$ , the number  $N$  of chains per in a unit volume, was deduced from the relation  $\mu = N k T$  [??]. The normalized radii that correspond to the maximum points of the two curves in Fig. 6 are  $\left(\frac{r}{nl}\right)_{n=50} \cong 0.1$  and  $\left(\frac{r}{nl}\right)_{n=100} \cong 0.075$  which and are compatible/consistent to with the analytical predictions  $\left(\frac{r}{nl}\right)_{n=50} = 0.115$  and  $\left(\frac{r}{nl}\right)_{n=100} = 0.082$ , respectively, given in section Sec. 3.2.3, of  $\left(\frac{r}{nl}\right)_{n=50} = 0.115$  and  $\left(\frac{r}{nl}\right)_{n=100} = 0.082$ , and presented/shown by the dashed columns in Fig. 6. The differences between the numerical and analytical results for the most probable end-to-end chain length is can be associated with the density of discretization of 0.025 for  $0 \leq \frac{r}{nl} \leq 1$ . Furthermore, it can be seen that the results of the current approach are different from the results  $\left(\frac{r}{nl}\right)_{n=50} = 0.141$  and  $\left(\frac{r}{nl}\right)_{n=100} = 0.1$ , obtained from of the random walk statistics of  $\left(\frac{r}{nl}\right)_{n=50} = 0.141$  and  $\left(\frac{r}{nl}\right)_{n=100} = 0.1$ , and presented by the dot-dashed columns in Fig. 6. The values of the Negative entropy that are smaller than zero are is irrational and is are truncated because as they it represents numbers of configurations that are in not compatible with the previously made assumption required for Stirling's approximation between that is applied to go from Eq. (21) and to Eq. (22).

(Note: the main idea - parameters value and initial calculations)

Next, for the purpose of evaluating the influences of to determine how f electrical excitation affects on the polymer structure during a polymerization process, different parameters were investigated as the electric-field magnitude ranged from  $0 \frac{\text{MV}}{\text{m}}$  to  $150 \frac{\text{MV}}{\text{m}}$ . The presented results are based on a numerical calculation where the number of monomers in a single chain, the length between the two contact points of a monomer with its neigh-

pics for experimental work 16.1.2020/ent vs r\_nl for

Figure 6: The entropy of a polymer chain with uniaxial dipoles as a function of the normalized radius as  $0 \leq \frac{r}{nl} \leq 1$  and  $l = 100 \mu\text{m}$ . The red continuous curve with circular markers corresponds to  $n = 50$  and the brown curve with squares to  $n = 100$ . The dashed columns corresponds to the normalized radii in accordance with the results in section 3.2.3,  $\frac{r}{nl} = \sqrt{\frac{2}{3}} \frac{1}{\sqrt{n}}$ , and the dot-dashed columns to the results from random walk statistics,  $\frac{r}{nl} = \frac{1}{\sqrt{n}}$ .

pics for experimental work 16.1.2020/LnOmega vs ElecField

Figure 7: The natural logarithm for the maximum number of configurations as a function of the electric field magnitude for chains with uniaxial dipoles at different inclinations. The blue curve with circular markers corresponds to  $\Theta = \frac{\pi}{1000}$ , the red curve with squares to  $\Theta = \frac{\pi}{4}$  and the yellow curve with diamonds to  $\Theta = \frac{\pi}{2}$ .

bors, and the number of chains perin a unit volume are the same as those ones assumed for the case of no electric field.

In order to demonstrate the influence of how electric fields with different of various magnitudes on affect chains at various inclinations with respect to the direction of the electric field, Figs. 7, 8, and 9 show results for chains with  $\Theta = \frac{\pi}{1000}$ ,  $\Theta = \frac{\pi}{4}$  and  $\Theta = \frac{\pi}{2}$ . are presented in Fig. 7, Fig. 8 and Fig. 9. Figure 7 shows the natural logarithm of the maximum number of configurations for each chain as a function of the electric field can be seen in Fig. 7, and Fig. 8 shows the end-to-end length with for the maximum number of configurations of each chain as a function of the electric field can be seen in Fig. 8. The Lagrange multiplier  $\tau$ , which can be portrayed may be understood as the chain's mechanical constraint and which, that is relateds to the end-to-end length of the chain with the maximum number of configurations, was is examined as a function of the electric-field magnitude, as can be seen in Fig. 9.

We note from Figs. 7, Fig. 8, and Fig. 9, that the magnitude results differ little for

pics for experimental work 16.1.2020/rad vs ElecField 29.

Figure 8: The most probable end-to-end length as a function of the electric field magnitude for chains with uniaxial dipoles at different inclinations. The blue curve with circular markers corresponds to  $\Theta = \frac{\pi}{1000}$ , the red curve with squares to  $\Theta = \frac{\pi}{4}$  and the yellow curve with diamonds to  $\Theta = \frac{\pi}{2}$ .

Figure 9: The size of the Lagrange multiplier  $\tau$ , associated with the most probable radius as a function of the electric field magnitude for chains with uniaxial dipoles at different inclinations. The blue curve with circular markers corresponds to  $\Theta = \frac{\pi}{1000}$ , the red curve with squares to  $\Theta = \frac{\pi}{4}$  and the yellow curve with diamonds to  $\Theta = \frac{\pi}{2}$ .

range of an electric field that is smaller less than  $50 \frac{\text{MV}}{\text{m}}$  has shown very small differences in results from the case of  $E = 0 \frac{\text{MV}}{\text{m}}$ . This is particularly evident in Fig. 8, where the change in the end-to-end length of the different chains is hardly visible below  $50 \frac{\text{MV}}{\text{m}}$ . In Figure 7 shows, we can observe the similarities in the curves for the natural logarithm of the maximum number of configurations for chains at different inclinations, which all decrease as the magnitude of the with increasing electric field is enhanced. The differences between the curves can be associated attributed to the number of end-to-end vectors in each inclination with respect to the direction of the electric field, as seen expected in from Eq. (120). By observing Figure 8, it can be seen shows that, with increasing electric field, the end-to-end length of chains at all inclinations increases as the magnitude of the electric field is enhanced. Though However, as the magnitude is enhanced electric field increases, the differences in the end-to-end length become more prominent, as because chains in at greater inclinations are longer. We find that this result is counterintuitive as because we would expect chains with greater inclinations with respect to the direction of the electric field to be shorter as because the monomers aspire tend to reorient in the direction of the electric field. From Figure 9 we can observe shows the differences in mechanical constraint of the chains mechanical constraint. As the magnitude of the With increasing electric field, is enhanced its value the constraint decreases for chains parallel to the direction of the the electric field and relatively increases somewhat for chains with at greater inclinations. This can be result is attributed to the fact that as the polymer being is in a solution state during the polymerization, and, it is "harder" to hold more energy is required to maintain chains at larger inclinations as the monomers react to the electric excitation and aspire to rotate towards its direction.

## 4.2 Monomers orientation

(Note: monomer distribution - chains)

Once the After calculating ons of the end-to-end lengths for chains at each of the mentioned as a function of inclination with respect to the direction of the electric field, [i.e., determining  $\mathbf{r}_j^0 = r^0(\Theta_j, \mathbf{E})\hat{\mathbf{r}}(\Theta_j)$ ], the monomers orientation can be calculated as

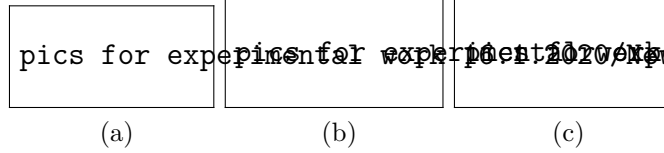


Figure 10: The monomer distribution for a polymer chain of uniaxial dipoles. The magnitude of the electric field during the polymerization process is  $E = 150 \frac{\text{MV}}{\text{m}}$ . (a) Corresponds to the chain with the inclination  $\Theta = \frac{\pi}{1000}$  and end-to-end length  $r = 0.89 \sqrt{n}l$ . (b) Corresponds to  $\Theta = \frac{\pi}{4}$  and  $r = 0.91 \sqrt{n}l$ . (c) Corresponds to  $\Theta = \frac{\pi}{2}$  and  $r = 0.93 \sqrt{n}l$ .

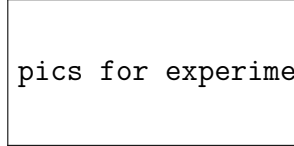


Figure 11: The amorphous monomer distribution of a uniaxial dipole as  $E = 150 \frac{\text{MV}}{\text{m}}$ . According to the numerical analysis as  $\tau = 0$  and identical to the results of the analytical analysis that was presented by ?.

detailed in [section Sec. 3.3.1](#). [Figures 10a\(a\), b and 10a\(c\)](#) [present show](#) the monomers distribution [offor](#) chains with [different](#) inclinations  $\Theta = \frac{\pi}{1000}$ ,  $\Theta = \frac{\pi}{4}$ , and  $\Theta = \frac{\pi}{2}$ , respectively, [while the magnitude of the and for an](#) electric field is  $E = 150 \frac{\text{MV}}{\text{m}}$ . In these three-dimensional plots, the length of the radius vector to each point represents the number of monomers aligned with [thisthe given](#) vector. [As can also be seenIn addition](#), the monomers distributions [are is compatibleconsistent](#) when comparing [between the](#) different inclinations. [This, which](#) means that the monomers in the different chains [aspiretend](#) to orient similarly. This [compatibilityconsistency](#) is very interesting, [as because](#) the chains have different inclinations and different end-to-end lengths.

**(Note: amorphous monomer distribution)**

[AsGiven that](#) the monomers orientation for each [of the mentionedgiven](#) chains [was is](#) obtained and their [likenesssimilarity is was](#) recognized, [the monomers we now examine](#) the monomer distribution in [anthe](#) amorphous case [is examined](#). [Figure 11](#) presents the results of [the](#) numerical calculations [forof the distribution of](#) amorphous monomers distribution [in the case offor](#) a uniaxial dipole [aaccording based on to](#) Eq. (42). Unlike [Figs. 10a, b and 10c](#), [Fig. 11](#) presents a symmetric distribution of [the](#) monomers, as in this case [thewhere](#) monomers are free to reorient separately and [are not be](#) constrained as [a](#) part of a chain. The result of the analytical analysis [forof](#) the PDF in the amorphous case [?], presented in Eq. (44), [can also be seenappears](#) in [Fig. 11 as theyand](#) are identical to the numerical results.

pics for experimental work 16.1.2020/Number of chain i

Figure 12: The number of chains along each inclination as a function of the inclination relative to the direction of the electric field,  $N(\Theta, \Phi = 0)$ . The blue curve with circular markers corresponds to the isotropic polymer and the yellow curve with squares corresponds to the biased polymer.

pics for experimental work 16.1.2020/weights comparison

Figure 13: The fractions of chains along each inclination as a function of the inclination to the direction of the electric field,  $\nu(\Theta)$ . The blue curve with circular markers corresponds to the isotropic polymer and the yellow curve with squares corresponds to the biased polymer.

### 4.3 The free state

(Note: finding the natural state - chains distribution, weights and lambda0 deformation)

After analyzing the micro-scale and understanding the monomer distribution as a result of the mentioned given polymerization process, we now examine the macro-scale is examined. Hence, as we wish to The analysis of the macroscopic response of the polymers to different excitations, as is detailed in section Sec. 3.4, requires an assessment of the relative influence of each of the chains groups in the different various inclinations needs to be assessed. For the sake of such evaluation This assessment is done by using Eqs. (116) and Eq. (120) are used to calculate the fraction of chains with the inclination  $j$ -th inclination with respect to the electric field. A Figure 12 compares the number of chains in of various the different inclinations with respect to the direction of the electric field between the for isotropic polymers and electric-field the-biased polymers is presented in Fig. 12, and Fig. 13 A comparison between the fractions of chains in each inclination for both each cases is presented in Fig. 13. The relations between the results shown in Figs. 12 and Fig. 13 are credited to  $\psi_j$ , which is the number of end-to-end vectors in the group  $j$ -th group, presented in as given by Eq. (120).

As can be observed from Figure. 12 shows that, the presence application of an external electric field induring the polymerization process affects the chain distribution of the chains, as the chains aspire to align in the direction of the electric field. Though However, Fig. 13 shows that, as a result because of Eq. (120) and as can be observed in Fig. 13, the most influential inclination of the polymer as a result of the proposed process is  $\Theta \cong \frac{\pi}{4}$ .

The density of discretization for To calculate the inclinations with respect to the direction of the electric field, the density of discretization is was taken as  $\Delta\Theta = \frac{\pi}{16}$ , as because denser discretizations diddo not produce any meaningful differences in significantly change

the results. ~~As w~~We refer to ~~the different~~ each individual groups of chains ~~discreetly~~ in accordance with their inclinations ~~with respect~~ to the ~~direction of the~~ electric field, and we attribute each ~~group~~ chains in each group ~~with~~ one end at the origin and the other end ~~located within~~ a small volume  $dV = r^2 dr d\phi d\theta$ . Furthermore, ~~we note that as~~because the DE coupling ~~in DEs~~ is ~~characterized by a~~ quadratic ~~dependence on their~~ applied electric potential [?], the different DE responses ~~of DEs~~ can be deduced ~~from~~by analyzing  $0 \leq \Theta \leq \frac{\pi}{2}$ . Accordingly, the groups that relates to inclinations  $\Theta = 0$  and  $\Theta = \frac{\pi}{2}$ , which are the boundaries of the analyzed range, are attributed to small volumes with  $\Delta\Theta = \frac{\pi}{32}$ . This is ~~performed done so as not~~ to avoid exceeding the limits set for the ~~tested~~ angular range ~~being tested~~.

~~Figure~~ 14 presents the analysis of the deformation  $\lambda_0$  of a polymer ~~in the direction~~ ~~of~~with respect to the electric field,  $\lambda_0$ , ~~of a polymer that was~~ induced during polymerization ~~with the chosen by the~~ electric-field magnitude ~~during the polymerization process~~, ~~as given that~~ the electric field is removed at the end of ~~the process~~polymerization. The chains are unable to ~~changetune~~ their lengths to ~~the length that~~ of the chains in the isotropic polymer ~~as because~~ they are cross-linked and cannot rearrange separately. Thus, each chain is affected by the same deformation gradient. The corresponding deformation gradient, while assuming incompressibility, is

$$\mathbf{F}^0(\lambda_0) = \lambda_0 \hat{\mathbf{E}} \otimes \hat{\mathbf{E}} + \frac{1}{\sqrt{\lambda_0}} (\mathbf{I} - \hat{\mathbf{E}} \otimes \hat{\mathbf{E}}) = \begin{pmatrix} \lambda_0 & 0 & 0 \\ 0 & 1/\sqrt{\lambda_0} & 0 \\ 0 & 0 & 1/\sqrt{\lambda_0} \end{pmatrix}. \quad (131)$$

~~In order to~~To assess the stress-free configuration of an incompressible body such as the biased polymer, ~~we examine various different~~ deformation gradients ~~were examined~~. ~~The A~~ suitable one is ~~depicted by~~obtained from the state where  $\sigma_{EE} = \sigma_{YY} = \sigma_{ZZ} = \frac{\text{Tr}(\sigma)}{3}$  ~~as because~~ the deviatoric stress is zero, in accordance with Eq. (19). As seen in Fig. 14,  $\lambda_0$  is achieved ~~from~~by calculating  $\sigma_{EE} - \sigma_{YY} = \sigma_{\text{Diff}}$  and determining the correct value from  $\sigma_{\text{Diff}}(\lambda_0) = 0$ . In this case, ~~it is received~~the correct value is ~~for~~  $\lambda_0 = 0.795$ , which means that the deformation gradient tensor ~~that is~~ compatible with the deformation after ~~the~~ removal of the electric field is

$$\mathbf{F}^0_{E=150 \frac{\text{MV}}{\text{m}}} = \begin{pmatrix} 0.795 & 0 & 0 \\ 0 & 1.121 & 0 \\ 0 & 0 & 1.121 \end{pmatrix}. \quad (132)$$

This ~~result~~ is counterintuitive when considering that, in this case, chains ~~in at~~ greater inclinations ~~will get~~become longer. ~~Though~~However, when considering the ~~monomer~~ orientation ~~of the monomers~~, it is reasonable to assume that some will ~~rearrange in grater~~become more inclination ~~ated~~ with respect to the electric field as it is removed. Thus, the polymer

pics for experimental work 16.1.2020/lambda 0 deformation

Figure 14:  $\sigma_{\text{Diff}} = \sigma_{\text{EE}} - \sigma_{\text{YY}}$  as a function of  $\lambda_0$  after the removal of the electric field with the magnitude of  $E = 150 \frac{\text{MV}}{\text{m}}$ .

pics for experimental work 16.1.2020/mechanical stress

Figure 15: The deviatoric mechanical stress as a function of the deformation ratio,  $\lambda$ . Dashed curves corresponds to the isotropic polymer, continuous curves to the biased polymer and the dot-dashed curves to a polymer described by the IED model. The blue curves corresponds to the normal stress in the direction of the electric field,  $\sigma_{\text{EE}}^{\text{m}}$ , and the red curves to the transverse stress,  $\sigma_{\text{YY}}^{\text{m}} = \sigma_{\text{ZZ}}^{\text{m}}$ .

will ~~perform~~undergo a planar expansion. The ~~chains~~ end-to-end lengths and inclination of the ~~chains~~ in the relaxed state, which from now on will be the starting point for each of the ~~chain~~ examined ~~chains~~ in thea biased polymer, can be deduced from  $\mathbf{r}_j = \mathbf{F}^0 \mathbf{r}_j^0$ . We also ~~n~~Note also that the same calculations for the isotropic case yielded  $\lambda_0^{\text{Iso}} = 1$ , as was expected.

#### 4.4 ~~M~~The materials properties

(Note: mechanical and electrostatic properties - new polymer + comparison)

AsGiven the chains orientations were established for the example mentioned ~~example~~, the properties of the biased polymer can be examined and compared ~~to~~with the case of an isotropic polymer, aswhich is detailed in ~~section~~Sec. 3.4.1. The polymer's mechanical properties can be assessed by evaluating the mechanical stresses as a function of the deformation ratio,  $\lambda$ , according to Eq. (124). The calculations of the mechanical stresses were ~~was~~ performed ~~done~~ by taking into account and averaging the stresses at  $0 \leq \Phi < 2\pi$  with a discretization of  $\Delta\Phi = \frac{\pi}{16}$  for each inclination  $\Theta$  with respect to the electric field,  $\Theta$ , and evaluating the stresses ~~in~~for each deformation ratio while taking into account the fractions of each inclination [(Eq. (116))] ~~in~~for each case of deformation. Figure 15 presents ~~t~~The mechanical stresses in the direction of the electric field and in the transverse plane as a function of the deformation ratio ~~are presented in Fig. 15~~ for the isotropic polymer, the biased polymer, and the IED model. -

The electrostatic properties can be assessed by first evaluating the polarization of the polymer as a function of the magnitude of the electric field. These calculations are performed ~~according to~~following the same steps ~~that were mentioned~~as for the stresses calculations. ~~F~~Figure 16 shows the susceptibilities of the biased polymer, isotropic polymer, and the IED model as a function of the electric field, ~~are presented in Fig. 16~~ as they

Figure 16: The susceptibilities of the polymers as a function of the electric field. The black dashed curve corresponds to the isotropic polymer, the black continuous curve to the biased polymer and the black dot-dashed line to a polymer described by the IED model. (the dashed and the continuous curves overlap).

are calculated according to using Eq. (129).

Figure 15A shows that applying an electric field during polymerization changes the stress. change in the stresses is visible in Fig. 15 as a result of the presence of an electric field in the polymerization process. More precisely, there is an increase in the stresses of the biased polymer increases, relatively to that of the isotropic polymer, both in the direction of the electric field and perpendicular to it. The stresses in the IED model are higher than exceeds that in both the of the other examined polymers examined.

Figure 16 shows that the biased polymer and the isotropic polymer have similar susceptibilities. for the biased polymer and the isotropic one. The susceptibilities of both the polymers are as the given initially similar susceptibility while under the excitation a weak of electric fields with small magnitudes (under less than  $E \cong 5 \frac{\text{MV}}{\text{m}}$ ) and they increase in values at almost identically identical rates as the magnitude of the electric field increases. We suspect that the resemblance similarity between the susceptibilities of the biased and isotropic polymers stems from the fact that, as the electric field is removed, at the end of our proposed process polymerization, the monomers aspires tend to rearrange rearrange as in the isotropic ease polymer while whereas the biased polymer deformed deforms. N We note that the numerical results of the determined susceptibility for of the biased polymer shows a slightly increases relatively to the isotropic polymer, although not enough for to visibly separation between the curves. The susceptibility of the IED model is not affected by independent of the magnitude of the electric field and is constant in value as the initial susceptibility. Hence These results indicate, it can be deduced that applying an electric field during polymerization the changes in the mechanical properties as a result of inducing the polymer with an electric field during the polymerization process are more prominent than those of the electrostatic properties.

## 4.5 The coupled response

(Note: coupled properties - new polymer + comparison)

After examining and comparing the mechanical and electrostatic properties, we also examine the coupled properties of the two biased and isotropic mentioned polymers can also be examined. For that this purpose, the main criterion to be examined is the defor-

Figure 17: The deformation in the direction of the electric field,  $\lambda$ , as a function of the magnitude of the electric field. The black dashed curve corresponds to the isotropic polymer, the black continuous curve to the biased polymer and the black dot-dashed curves to a polymer described by the IED model.

mation,  $\lambda$ , as a function of the magnitude of the induced applied electric field, presented in (see Fig. 17). As can be seen shown in Fig. 17, the deformations of the biased polymer are smaller than those of the isotropic polymer. These results agree are consistent with the previous ones results. As it was established from Figure 16 establishes that the electrostatic response of the biased polymer shows no meaningful does not difference significantly from that of the isotropic polymer, from and Fig. 15 it can be interpreted shows that the biased polymer is stiffer than the isotropic polymer. Furthermore, as the susceptibility of the IED model is constant and generally smaller in value than for both the other polymers within the examined magnitude range of electric fields examined, so the stresses in the IED model are higher than exceeds that in both the other polymers. Thus, it is logical that the deformations of the IED model are the smallerst of the three than those in the biased and isotropic polymers.

## 5 Experimental work

Additionally, a deeper understanding of the electromechanical properties of polymers is required beyond what is provided by our analytical and numerical work. ~~as deeper understanding of the polymers coupled electromechanical behavior is required.~~ Therefore, we now present ~~Experimental studies aimed toward~~ that examining the coupled response of ~~different~~ various DEs such as VHB and PDMS ~~are also being performed~~ and compare ~~their results~~ to analytical calculations. The dielectric constant of the DEs is first determined ~~by firstly determining~~ by calculating the relative permittivity from the capacitance of capacitors ~~with containing~~ these DEs as their medium, ~~from which the relative permittivity can be calculated.~~ A common method used to ~~carry out~~ make such measurements is based on the analysis of the capacitance component in an LCR (~~L-inductance, C-capacitance, R-resistance~~) circuit by means of an LCR meter or a ~~simpler versions of this instrument,~~ the capacitance meter.

The ~~presented~~ experimental work ~~presented below~~ is divided to two main parts: The first ~~part~~ includes an ~~expansion~~ extension of the work presented in ? and examines ~~the influence of how the~~ uniaxial and biaxial stretching ~~on affects~~ the dielectric constant. The second ~~part includes the first~~ presentation of a new experimental system ~~which is aimed towards~~ for measuring the dielectric constant of polymers under an electric field ~~are reports the results for.~~ The two polymers: ~~that were chosen to be examined are~~ VHB 4910 (a commercially available acrylic elastomer ~~by from~~ 3M) and ~~p~~Polydimethylsiloxane (PDMS, that ~~was~~ made in our lab ~~from by~~ using the Dow Corning Sylgard 182 Silicone Elastomer Encapsulation Kit). These materials are of interest ~~due to~~ for their flexibility and accessibility.

### 5.1 The influence of uniaxial and biaxial stretching

The first experimental system we present allows us to evaluate ~~the influence of how~~ uniaxial and biaxial stretching of DEs ~~on affects~~ their dielectric constant and to deepen the examination of the dependence of the dielectric constant on ~~the~~ deformation. The experimental system ~~is was~~ built from a self-constructed stretching device with four movable grippers, ~~as can be seen shown~~ in Fig. 18a. ~~In order to~~ To measure the relative permittivity of the deformed samples, a C-shaped clamp ~~is used serving~~ as a plate capacitor (Fig. 18b) ~~and is was~~ connected to an ~~capacitance meter,~~ Agilent U1701A ~~capacitance meter.~~ The experimental relative permittivity of each sample is calculated ~~via by~~ using

$$\epsilon_{r_{Exp}} = \frac{C_s d}{A \epsilon_0}, \quad (133)$$

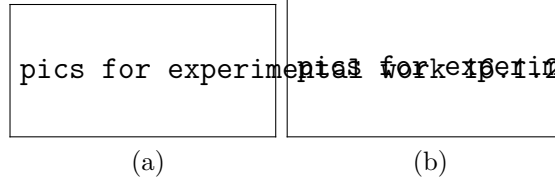
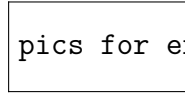
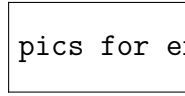


Figure 18: (a) The self constructed stretching device. (b) The C-clamp used as a parallel plate capacitor.



(a)



(b)



(c)

Figure 19: The relative permittivity measurements as functions of the percentage of surface area expansion. The dashed and dotted curves correspond to the analytical results [?], as  $n$  are estimated from the stretch at failure ( $n_f$ ) and from fitting the analytical equations to the experimental results ( $n_e$ ), respectively. (a) PDMS under uniaxial stretch. (b) VHB under uniaxial stretch. (c) VHB under biaxial stretch.

where  $C_s$  is the measured capacitance,  $d$  and  $A$  are the thickness and surface area of the capacitor, respectively, and  $\epsilon_0$  is the vacuum permittivity. The analytical relative permittivity for uniaxial stretching of the dielectric elastomers is calculated via by using ?

$$\epsilon_{rU} = 1 + \chi_0 \left[ 1 - \frac{1}{5n} \left( \lambda^2 - \frac{1}{\lambda} \right) \right]. \quad (134)$$

The calculation for the analytical relative permittivity was extracted is calculated in the current work herein based on from the results of ? for the case of biaxial stretchings.

The final expression is

$$\epsilon_{rB} = 1 + \chi_0 \left[ 1 - \frac{2}{5n} \left( \lambda^2 - \frac{1}{\lambda^4} \right) \right], \quad (135)$$

where  $n$  is the number of monomers in a single chain,  $\chi_0$  is the initial susceptibility, and  $\lambda$  is the magnitude of the uniaxial or biaxial stretchings.

Figure 19 he presents the results of the experiments and the analytical calculations for of the relative permittivity as a function of the percentage of surface area expansion are presented in Fig. 19 for uniaxial stretching of PDMS (Fig. 19a), uniaxial stretching of

Table 1: The number of monomers in a single chain for the case presented in Fig. 19.

	PDMS - Uniaxial	VHB - Uniaxial	VHB - Biaxial
$n_f$	4.35	80	80
$n_e$	5.844	21.807	5.156

VHB 4910 (Fig. 19b), and for biaxial stretching of VHB 4910 (Fig. 19c). The analytical results for uniaxial and biaxial stretching are also presented for the different cases examined. The number of monomers in a single chain is estimated from the stretch at failure, which is presumed to be the lock-up stretch, and is labeled as  $n_f$ , and from fitting the analytical equations to the experimental results as  $n_e$ , as is shown in Table 1.

As can be observed, the results show that while stretching the samples are stretched and decreases their thickness decreases their relative permittivity decreases. The incompressibility assumption was also examined and, in the case of the for PDMS, the results of both the measured and the calculated thickness can be observed are shown. The incompatibility of the curves based on the number of monomers in a polymer chain from the stretch at failure can may stem from the fact that the stretch at failure is not necessarily the lock-up stretch of the chain.

## 5.2 The influence of an electric field

The goal of this is experimental work is aimed was toward to examining the effect of how electric fields with of varying different magnitudes on affect the dielectric properties of various polymers. For that purpose Toward that end, we will present a new experimental system which that allows us to evaluate the variations of their dielectric constant as a function of applied electric field is applied on them. Furthermore, we will continue the work performed in of ? and deepen the examination of the dependence of how the dielectric constant depends on the deformation by performing our examination examining on pre-stretched samples.

### 5.2.1 Experimental set-up

(Note: Samples description)

(Note: Presenting the experimental system)

Ten rectangular samples of each of the two chosen polymers were cut for each examined easeation. For the ease of the pre-stretched VHB, the samples were then stretched by using a self-constructed stretching apparatus comprised consisting of two movable grippers, as can be seen shown in Fig. 18a.

pics for experimental work 16.1.2020/drawing of the s

Figure 20: A schematic description of the experimental system.

pics for experimental work 16.1.2020/electrodes and gr

Figure 21: The parts of the plate capacitore.

~~Our new~~This experimental system ~~is was~~ built from non-conductive materials, ~~all but~~ except for the two ~~30-mm-diameter~~ electrodes ~~with a diameter of 30 mm~~ that ~~are were~~ made ~~from of~~ copper and acted as one of two capacitors connected in ~~a row~~series, as ~~can be seen shown~~ in Fig. 20. The two electrodes ~~are were~~ each held in a ~~60-mm-diameter~~ Teflon housing ~~with a 60 mm diameter~~, as ~~can be seen shown~~ in Fig 21. ~~As t~~The medium in the ~~mentioned~~ plate capacitor ~~is contained~~ the ~~examined~~ elastomer sample under examination, and the second capacitor ~~is a capacitor with a fixed capacitance, which can be regarded as consisted of~~ a fixed TDK UHV-241A capacitor. ~~For the current work a ceramic capacitor suitable for high voltage is used, TDK's UHV-241A.~~

~~For the ease of~~To examine ~~ing~~ pre-stretched samples, we first used a bi-directional stretching apparatus ~~in order~~ to generate the required tension. After ~~the~~ stretching, the sample ~~is was~~ held in the stretched state by using a two-~~parts~~ self-constructed Perspex gripper with a ~~60-mm-diameter~~n opening ~~of 60 mm diameter~~ in the middle and an O-ring notch to maintain the tension in the sample, as ~~can be seen shown~~ in Fig. 21.

~~In order t~~To measure the referential permittivity of the different samples, we ~~make~~ used ~~of~~ the plate capacitor from ~~our the~~ experimental system. This measurement ~~is performed was made~~ by connecting ~~it the~~ plate capacitor to a capacitance meter before ~~connecting~~ the experimental system ~~is connected~~ to the power source. Furthermore, the distance between the electrodes ~~is was~~ measured in each experiment. After ~~obtaining~~ the referential values ~~are obtained~~, the power source ~~is was~~ connected to the ~~described~~ experimental system. As the supplied potential difference is changed in the power source. ~~t~~The potential difference ~~on across~~ the plate capacitor ~~is was~~ measured as a function of the potential difference applied by the power source by using a non-contact ~~voltmeter~~, USSVM2 volt-meter ~~by from~~ AlphaLab.

(Note: Presenting the work method or protocol)

~~For the purpose of~~To evaluate ~~ing~~ the relative permittivity of the polymer ~~while under an~~ under electrostatic excitation, ~~the conservation of charge conservation~~ is taken into account as follows;

$$Q = C_s V_s = C_0 V_0, \quad (136)$$

pics for experimental work 16.1.2020/PDMS RESULTS 24.

(a)

pics for experimental work 16.1.2020/VHB un and pre s

(b)

Figure 22: The permittivity measurements as functions of the electric field on the sample. The Blue dots corresponds to a relaxed sample and the red circles corresponds to the area pre-stretch of  $A = 225\%$ . (a) PDMS, (b) VHB.

where  $Q$  is the charge on ~~both of the~~ each capacitors,  $V_s$  and  $C_s$  are the potential difference across and the capacitance of the examined polymer, and  $V_0$  and  $C_0$  are the potential difference across and the capacitance of the fixed capacitor. Thus,

$$V_t = V_s + V_0 = Q \left( \frac{1}{C_s} + \frac{1}{C_0} \right), \quad (137)$$

where  $V_t$  is the total potential difference ~~as it is~~ supplied ~~from~~ by the power source. ~~While taking into account Equation-~~ (137) ~~we can obtain the relation,~~ gives

$$C_s = \left( \frac{V_t}{V_s} - 1 \right) C_0, \quad (138)$$

from which the current capacitance of the polymer can be calculated, while the constant ~~value of~~  $C_0$  is ~~taken~~ determined by the ~~from its~~ data shift and confirmed at the beginning of ~~the~~ each experiment ~~with~~ by measurements made with the capacitance meter.

The relative permittivity, which is the electrostatic property ~~that we aim to examine under investigation~~, is calculated from the results of the ~~calculated~~ capacitance ~~calculations~~ by using ~~the relations presented in~~ Eq. (133).

## 5.2.2 Results and discussion

In all tests, the ~~sample~~ thickness ~~of the samples were~~ was measured ~~for~~ in order to the ~~calculation of~~ the relative permittivity, ~~presented in~~ by using Eq. (133) ~~and thereby,~~ and ~~the~~ correctly ~~assessment~~ determine ~~of~~ the electric field ~~that is~~ induced ~~on~~ in the sample, which is calculated as  $E_s = \frac{V_s}{d}$ . ~~Measurements of~~ the pre-stretched VHB 4910 ~~have led to the understanding that~~ confirmed the incompressibility assumption ~~is reasonable and can be employed~~ in this case.

~~In~~ The solid blue dots (red open circles) in the two plots of Fig. 22 show, the measured relative permittivity ~~measurements~~ as a functions of the electric field ~~on the samples for~~ in

the un-stretched samples ~~are marked by blue filled dots and for the~~ (2.25 area pre-stretched samples ~~by red empty circles~~). The error bars show the standard deviations ~~are marked by error bars~~. ~~An agreement between~~ The results shown in ~~section~~ Sec. 5.1 are consistent with ~~and~~ the current results ~~can be identified in cases where~~ as  $E_s \rightarrow 0$ . ~~In the case of~~ For the VHB 4910 samples (Fig. 22b), the relatively small standard deviations of the different measurements provides confidence in the accuracy of the measurements for this material. The relatively larger standard deviations of the PDMS samples ~~can be as a result of~~ may be attributed to the fact that the samples were made manually in our lab, although ~~there is~~ a clear trend ~~appears~~ in the results. ~~We find that~~ The relative permittivity of the two ~~examined~~ polymers ~~examined~~ increases with the magnitude of the electric field.

The variations in the responses of the two ~~examined~~ polymers ~~examined~~ hints that these are governed by the ~~polymer~~ microstructure ~~of the polymers~~. Furthermore, the results of the pre-stretched VHB 4910 ~~another~~ provides more evidence ~~to~~ of the ~~governing~~ role of the microstructure ~~can be seen in the results of the pre-stretched VHB 4910~~. As ~~Given that~~ the initial values of the relative permittivity corresponds to the results ~~in~~ shown in Fig. 19, the maximum relative permittivity measured in the pre-stretched case is much ~~lower than~~ less than the ~~one~~ that measured in the relaxed case, despite the fact that ~~we achieved larger magnitudes of a~~ stronger electric field ~~was achieved as~~ in the ~~thickness of the~~ thinner samples ~~was decreased~~. ~~It can be seen in~~ The results for both the polymers (Fig. 22) show that, the rate of change in relative permittivity ~~deviation~~ is much ~~steeper~~ greater ~~in~~ at relatively low electric fields ( $< 1 \frac{\text{MV}}{\text{m}}$ ). Thus, additional experimental analyses of the relationship between the microscopic structure and the macroscopic response are needed ~~for the~~ to understanding of the coupled electromechanical behaviors of different polymers.

## 6 Conclusions

(Note: Opening - Motivation)

~~Although~~ This thesis presents another possible step towards the realization use of the DEs ~~potential for being used~~ in a wide range of applications ~~and~~, it comes at a time when ~~our culture is~~ we are seemingly ready for such advances in different fields, such as clean energy, medicine, and robotics. ~~Hence~~ Thus, ~~as given that~~ a substantial improvement in the electromechanical response of DEs is ~~needed~~ required, we present a possible method for influencing and analyzing the response of these materials and their structure and properties ~~of the polymer~~, all without adding any foreign materials.

(Note: 3. Electroelasticity of solutions and anisotropic networks of polymer molecules)

(Note: 3.1 general - multiscale analysis)

~~Initially~~ To begin, we carried out a multiscale analysis of the electromechanical coupling in DEs ~~at~~ for several hierarchical cases, from a single electric charge to a network. The analysis ~~accounts for the~~ applies the conservation of energy through the first law of thermodynamics, in terms of the electric enthalpy and the entropy of a system ~~that is~~ subjected to an electric field. ~~Our~~ The analysis of the polymer microstructure ~~of the polymer~~ is based on statistical mechanics, ~~as~~ and we assume that ~~the configuration of~~ each chain is in the ~~one that was calculated as~~ most probable configuration.

(Note: 3.2 an analysis of the isotropic chain end-to-end length, tau and force)

We ~~carry out an~~ analyze ~~of~~ the polymer chain, in the case of no electric field. This analysis yielded the relationship between the Lagrange multiplier  $\tau$ , which can be ~~portrayed~~ understood as the chain's mechanical constraint, and the normalized end-to-end length of the chain through the Langevin function. ~~Our~~ The calculations also ~~yielded an assessment~~ determine for the end-to-end length of a chain in such a case, which is similar to the ~~one~~ obtained by ?? and ? but ~~different from~~ than the commonly used ~~assessment given~~ result based on ~~from~~ random walk statistics [???]. ~~A~~ In addition, we deduce a relation between the end-to-end length of a chain and the external force ~~operating~~ exerted on ~~it~~ ~~was also deduced~~ the chain.

(Note: 3.3 polymer chains in an electric field and monomers distribution)

~~As our~~ To examine the proposed method for controlling the electro-elastic modulus of a polymer network by ~~executing the~~ polymerization ~~processing~~ under an electric field ~~is examined~~, we ~~describe a manner for the assessment~~ develop an approach to determine of the most probable configurations for each ~~of the~~ group of polymer chains ~~groups~~ and for the orientational distribution of ~~for~~ the monomers ~~orientational distribution~~ in such a case.

(Note: 3.4 an anisotropic network analysis - general analysis with a reference for polymerization under an electric field + material properties)

Next, we derive an expression ~~is derived~~ for the total entropy of the polymer ~~which that~~ allows us to evaluate the distribution and the fractions of the chains in the different chains groups. ~~Next, once~~ Given these ~~the~~ fractions ~~of the chains in the different groups were determined~~, expressions for the mechanical stress and the polarization ~~were~~ are derived in order to determine the polymer response ~~of the polymer~~.

(Note: 4. Application to electrostatically biased network - remind our main idea for the polymerization)

To examine the outcome of our proposed ~~process of~~ polymerization under an electric field, ~~that which~~ leads to a “biased” polymer, we applied a numerical analysis ~~was performed~~. ~~This analysis is an application of~~ based on our analytical work, and ~~its~~ the predictions of this analysis are ~~is~~ compared with the experimental results for an isotropic polymer and for the IED model.

(Note: 4.1 chain end-to-end length - isotropic case (our analysis is more accurate) and anisotropic (mention the examined parameters))

The initial step of the numerical analysis involves ~~an examination of our assessment~~ the results for the end-to-end length of a chain in ~~the case of~~ an isotropic polymer. ~~In regards to the configuration of the chains in~~ For the biased polymer, ~~a comparison~~ the chain configuration ~~was performed~~ is compared for three parameters: the maximum number of chain configurations ~~of the chain~~, the most probable end-to-end length, and the Lagrange multiplier  $\tau$  that relates to the end-to-end length ~~with~~ to the maximum number of configurations. ~~From which~~ The results indicate ~~we determined~~ that magnitude ~~ranges of~~ the electric fields ~~lower~~ less than  $50 \frac{\text{MV}}{\text{m}}$  ~~have shown hardly any~~ produce negligible differences ~~in results from~~ with respect to the isotropic case. ~~Though~~ However, ~~when enhancing the magnitude further~~ upon increasing the electric field, the end-to-end length of chains ~~in~~ increases for all inclinations ~~increases~~, which is counterintuitive ~~as~~ because ~~the~~ uniaxial dipolar monomers ~~aspire~~ tend to rotate ~~towards~~ in the direction of the electric ~~excitation~~ field.

(Note: 4.2 monomer orientation - aspire to be as in the amorphous case)

The ~~findings from the examinations~~ results of the investigation of the monomers orientation for chains ~~in the different~~ at various inclinations with respect to the electric field and the comparison ~~to~~ with the monomer distribution ~~of monomers~~ in the amorphous case ~~led to the realization~~ shows that, despite their constraints, ~~the~~ monomers in ~~the~~ chains ~~aspire~~ tend to orient as though they ~~are~~ were unattached.

(Note: 4.3 assessing the free state and discussing the chains distribution/weights)

Next, the free state of the biased polymer was assessed. This state ~~occurs~~ is achieved when the deviatoric stress vanishes and the body is ~~at~~ in a stress-free configuration. ~~It was found~~ The results show that the biased polymer contracts in the direction of the applied electric field, ~~which~~. ~~This~~ ~~strengthens~~ improves our understanding of the importance to

polymer properties of the microscopic structure ~~to the properties of the polymer, since~~ because, when the electric field is turned off, the monomers rotate away from its direction ~~and hence the,~~ which leads to contraction in ~~that~~ the given direction. The spatial expansion in the transverse direction is due to incompressibility.

(Note: 4.4 the material properties and coupled response)

The resulting material properties ~~shows a difference between~~ from the mechanical ~~ones~~ properties, as manifested by the biased polymer ~~is found to be~~ being stiffer than the isotropic ~~one~~ polymer. ~~Regarding the electrostatic properties, n~~ No significant differences in the electrostatic properties ~~are~~ were found between the two polymers. ~~Though~~ However, in both cases the susceptibility ~~does not~~ appears to ~~be fixed~~ vary under different magnitudes ~~of~~ as a function of electric ~~field~~ magnitudes. The analysis of the coupled response establishes that the electromechanical response of the biased polymer is less than that of the isotropic polymer, which is consistent ~~In accordance~~ with the ~~assessed~~ mechanical and electrostatic properties of both polymers. ~~from the analysis of the coupled response, it was established that the electromechanical response of the biased polymer is smaller than the isotropic polymer.~~

(Note: 5. Experimental work)

The ~~findings~~ results of ~~our~~ the present experimental work imply that the dependence of the ~~polymers~~ dielectric properties ~~of the polymers~~ on the deformation and the ~~electric-field~~ magnitude ~~of the electric field~~ cannot be neglected. Moreover, they suggest that common models that assume constant relative permittivity, such as the models of ? and ?, are not applicable if the polymer is subjected to different mechanical loads or ~~excitations~~ ~~from~~ exposed to an electric fields at different magnitudes. Additionally, ~~we observed that~~ our extension to the model of ? for the case of biaxial stretchings ~~is able to~~ predicts the relationship between ~~the~~ relative permittivity, which ~~represents~~ reflects the dielectric behavior, and ~~the polymer~~ deformation ~~of the polymer~~. ~~Though~~ However, the assessment of the number of monomers in a single chain from the stretch at failure ~~does not yield a good enough~~ is insufficient to prediction of these mentioned relationships, which. This ~~can~~ may stem from the fact that the stretch at failure is not necessarily the lock-up stretch of the chain. Furthermore, ~~from~~ our examination of ~~the effect of~~ how electric fields ~~with different~~ of varying magnitudes ~~affect~~ on the dielectric properties; ~~reveals~~ the differences in the responses of the relaxed and pre-stretched VHB 4910, ~~thereby demonstrating~~ the prominent influence of the microscopic structure on the macroscopic electromechanical behavior. Accordingly, ~~it can be seen that~~ pre-stretching the sample ~~is found to~~ hinders the evolution of the relative permittivity as the magnitude of the electric field increases.

(Note: \*\* Future work)

We have spent considerable time pondering the future directions of this research. ~~While~~ Although this thesis presents ~~a~~ method of ~~influencing~~ tuning polymer ~~the~~ proper-

ties of polymers, so far it has so far been applied only to the case of uniaxial dipoles. Thus, an analysis should be performed for spontaneous and transversely isotropic dipoles should also be analyzed as well. In addition, the creation of a biased polymer should be examined from different directions and with electric fields of greater magnitudes of electric fields in order to assess/determine the threshold field from above which there are significant differences appear in the electrostatic properties in comparison with the *à vis* the isotropic polymer. Moreover, from the experimental perspective, the influence of how an electric field affects on the dielectric properties should be experimentally examined for additional materials, with more pre-stretching conditions and under higher magnitudes of electric fields.

## References

# Appendix

## A Presentation of the first law of thermodynamics in terms of electrical enthalpy

The first law of thermodynamics is  $\dot{U} = \dot{W}_0 + \dot{Q}$  [(Eq. (7))], where

$$\dot{U} = \frac{d}{dt} \int_{V_0} u(\mathbf{F}, \mathbf{P}) dV_0 + \frac{d}{dt} \int_{\mathbb{R}^3} \frac{\epsilon_0}{2} \mathbf{E} \cdot \mathbf{E} dV, \quad (139)$$

and where the system is assumed to not to interactions-between-the-system-andwith other bodies and that-far-away the electric fields is assumed to vanish are-assumedfar from the system. The rate of work done by the mechanical loads due-tothrough deformation and by the electric field due-tothrough variations in the charge is [??]

$$\frac{dW_0}{dt} = \int_V b_i v_i dV + \int_{\partial V} t_i v_i dA + \int_V \phi \frac{d}{dt} (q dV) + \int_{\partial V} \phi \frac{d}{dt} (\rho_a dA). \quad (140)$$

We recall Using the definition of the electric enthalpy density [?],

$$h(\mathbf{F}, \mathbf{E}) = u(\mathbf{F}, \mathbf{P}) - \mathbf{J} \mathbf{P} \cdot \mathbf{E}, \quad (141)$$

Accordingly gives

$$\begin{aligned} \dot{U} &= \frac{d}{dt} \int_{V_0} h(\mathbf{F}, \mathbf{E}) dV_0 + \frac{d}{dt} \int_{V_0} \mathbf{P} \cdot \mathbf{E} J dV_0 + \frac{d}{dt} \int_{\mathbb{R}^3} \frac{\epsilon_0}{2} \mathbf{E} \cdot \mathbf{E} dV \\ &= \frac{d}{dt} \int_{V_0} h(\mathbf{F}, \mathbf{E}) dV_0 + \frac{d}{dt} \int_V \mathbf{P} \cdot \mathbf{E} dV + \frac{d}{dt} \int_{\mathbb{R}^3} \frac{\epsilon_0}{2} \mathbf{E} \cdot \mathbf{E} dV. \end{aligned} \quad (142)$$

Since i In the body  $\mathbf{D} = \mathbf{P} + \epsilon_0 \mathbf{E}$  and outside the body  $\mathbf{D} = \epsilon_0 \mathbf{E}$ , so

$$\dot{U} = \frac{d}{dt} \int_{V_0} h(\mathbf{F}, \mathbf{E}) dV_0 + \frac{d}{dt} \int_{\mathbb{R}^3} (\mathbf{D} - \epsilon_0 \mathbf{E}) \cdot \mathbf{E} dV + \frac{d}{dt} \int_{\mathbb{R}^3} \frac{\epsilon_0}{2} \mathbf{E} \cdot \mathbf{E} dV. \quad (143)$$

Thus, we have that

$$\dot{U} = \frac{d}{dt} \int_{V_0} h(\mathbf{F}, \mathbf{E}) dV_0 - \frac{d}{dt} \int_{\mathbb{R}^3} \frac{\epsilon_0}{2} \mathbf{E} \cdot \mathbf{E} dV + \frac{d}{dt} \int_{\mathbb{R}^3} \mathbf{D} \cdot \mathbf{E} dV. \quad (144)$$

Define  $\dot{H} = \frac{d}{dt} \int_{\Omega_0} h(\mathbf{F}, \mathbf{E}) dV_0$  as the stored electric enthalpy in the body. According to-tThe first law of thermodynamics then gives

$$\dot{H} - \frac{d}{dt} \int_{\mathbb{R}^3} \frac{\epsilon_0}{2} \mathbf{E} \cdot \mathbf{E} dV = \dot{W}_0 + \dot{Q} - \frac{d}{dt} \int_{\mathbb{R}^3} \mathbf{D} \cdot \mathbf{E} dV. \quad (145)$$

Consider the last term

$$-\frac{d}{dt} \int_{\mathbb{R}^3} \mathbf{D} \cdot \mathbf{E} dV = \frac{d}{dt} \int_{\mathbb{R}^3} \mathbf{D} \cdot \nabla \phi dV = \frac{d}{dt} \int_{\mathbb{R}^3} \nabla \cdot (\mathbf{D}\phi) dV - \frac{d}{dt} \int_{\mathbb{R}^3} \nabla \cdot \mathbf{D} \phi dV. \quad (146)$$

Assuming no free charges outside the body, then  $\nabla \cdot \mathbf{D} = q$  in the body and zero outside, so

$$-\frac{d}{dt} \int_{\mathbb{R}^3} \mathbf{D} \cdot \mathbf{E} dV = \frac{d}{dt} \int_{\partial V} \phi \mathbf{D} \cdot \hat{\mathbf{n}} dA - \frac{d}{dt} \int_V \phi q dV, \quad (147)$$

where we make use of the divergence theorem and exploit the assumption that **far-enough** the electric field vanishes **at distance**. Thus,

$$-\frac{d}{dt} \int_{\mathbb{R}^3} \mathbf{D} \cdot \mathbf{E} dV = -\frac{d}{dt} \int_{\partial V} \phi \rho_a dA - \frac{d}{dt} \int_V \phi q dV. \quad (148)$$

The last term can be simplified to

$$\begin{aligned} -\frac{d}{dt} \int_V \phi q dV &= -\frac{d}{dt} \int_{V_0} \phi q J dV_0 = -\int_{V_0} \dot{\phi} q J dV_0 - \int_{V_0} \phi \frac{d}{dt} (q J dV_0) \\ &= -\int_V \dot{\phi} q dV - \int_V \phi \frac{d}{dt} (q dV). \end{aligned} \quad (149)$$

The first term of Eq. (148) is,

$$-\frac{d}{dt} \int_{\partial V} \phi \rho_a dA = -\frac{d}{dt} \int_{\partial V_0} \phi \rho_a^0 dA_0, \quad (150)$$

where  $\rho_a^0$  is the referential surface charge such that  $\rho_a^0 dA_0 = \rho_a dA$ . Thus,

$$-\frac{d}{dt} \int_V \phi q dV = -\int_{\partial V_0} \dot{\phi} \rho_a^0 dA_0 - \int_{\partial V_0} \phi \frac{d}{dt} (\rho_a^0 dA_0) = -\int_{\partial V} \dot{\phi} \rho_a dA - \int_{\partial V} \phi \frac{d}{dt} (\rho_a dA). \quad (151)$$

Substituting **this relation into** Eq. (148) **we have gives**

$$-\frac{d}{dt} \int_{\mathbb{R}^3} \mathbf{D} \cdot \mathbf{E} dV = -\int_{\partial V} \dot{\phi} \rho_a dA - \int_{\partial V} \phi \frac{d}{dt} (\rho_a dA) - \int_V \dot{\phi} q dV - \int_V \phi \frac{d}{dt} (q dV), \quad (152)$$

**Substituting and using this relation into** the first law of thermodynamics, [Eq. (145)], **with the use of** and the expression for the external work  $W_0$  [Eq. (140)], **we have gives**

$$\begin{aligned} \dot{H} - \frac{d}{dt} \int_{\mathbb{R}^3} \frac{\epsilon_0}{2} \mathbf{E} \cdot \mathbf{E} dV &= \int_V \phi \frac{d}{dt} (q dV) + \int_{\partial V} \phi \frac{d}{dt} (\rho_a dA) + \dot{Q} + \int_V b_i v_i dV + \int_{\partial V} t_i v_i dA \\ &\quad - \int_{\partial V} \dot{\phi} \rho_a dA - \int_{\partial V} \phi \frac{d}{dt} (\rho_a dA) - \int_V \dot{\phi} q dV - \int_V \phi \frac{d}{dt} (q dV) \\ &= \dot{Q} - \int_{\partial V} \dot{\phi} \rho_a dA - \int_V \dot{\phi} q dV + \int_V b_i v_i dV + \int_{\partial V} t_i v_i dA. \end{aligned} \quad (153)$$

In terms of the external work due to the variations in the electric potential [??],

$$\frac{dW}{dt} = \int_V b_i v_i dV + \int_{\partial V} t_i v_i dA - \int_{\partial V} \dot{\phi} \rho_a dA - \int_V \dot{\phi} q dV, \quad (154)$$

we **endfinally obtain**-with the expression for the first law of thermodynamics in terms of the electric enthalpy:

$$\dot{H} - \frac{d}{dt} \int_{\mathbb{R}^3} \frac{\epsilon_0}{2} \mathbf{E} \cdot \mathbf{E} dV = \dot{W} + \dot{Q}. \quad (155)$$

## B Chain stress and deriving the chain end-to-end vector ~~by~~from the deformation gradient

~~In order to~~To evaluate the stress, ~~depicted~~(see discussion in ~~section~~Sec. 3.4.1), we first ~~derivation of~~ the term  $\frac{\partial \mathbf{r}}{\partial \mathbf{F}}$  ~~is needed~~. This is ~~carried out~~done ~~in using~~ index notation.

The end-to-end vector of the chain in the current configuration is

$$\mathbf{r}_i = F_{ip} \mathbf{r}_p, \quad (156)$$

where  $\mathbf{r}_i^0$  is the end-to-end vector of the chain in the reference configuration and  $F_{ij}$  is the deformation gradient. Accordingly,

$$\frac{\partial r_i}{\partial F_{kl}} = \frac{\partial}{\partial F_{kl}} (F_{ip}) r_p^0 = \delta_{ik} \delta_{lp} r_p^0 = \delta_{ik} r_l^0. \quad (157)$$

From Eq. (124), the mechanical stress in ~~the~~chain ~~j-th~~chain is

$$\sigma_{ks}^{m(j)} = \frac{kT}{l} \left( \tau_i^{(j)} \frac{\partial r_i^{(j)}}{\partial F_{kl}} \right) F_{sl} = \frac{kT}{l} \tau_i^{(j)} \delta_{ik} \delta_{lp} r_p^{0(j)} F_{sl} = \frac{kT}{l} \tau_k^{(j)} F_{sp} r_p^{0(j)} = \frac{kT}{l} \tau_k^{(j)} r_s^{(j)}. \quad (158)$$

Since  $\tau_k^{(j)} \parallel r_s^{(j)}$  (established in ~~section~~Sec. 3.2.3), it follows that

$$\sigma_{ks}^{m(j)} = \frac{kT}{l} \tau^{(j)} r^{0(j)} \hat{r}_k^{(j)} \hat{r}_s^{(j)}. \quad (159)$$

## C The initial guess for $\boldsymbol{\tau}$

The Lagrange multiplier  $\boldsymbol{\tau}$  is extracted from the implicit equation that follows from the constraint ~~is~~ given by Eq. (98),

$$\int \hat{\boldsymbol{\xi}} p d\Gamma = \frac{\mathbf{r}}{nl}, \quad (160)$$

where

$$p(\hat{\boldsymbol{\xi}}, h) = \frac{1}{Z} \exp\left(\boldsymbol{\tau} \cdot \hat{\boldsymbol{\xi}} - \frac{h}{kT}\right). \quad (161)$$

Taking the first two terms of the Taylor-series expansion ~~series~~ for  $\boldsymbol{\tau}$  gives

$$\boldsymbol{\tau} = \boldsymbol{\tau}_0 + \mathbf{A}\mathbf{r} + o(r^2) \cong \mathbf{A}\mathbf{r}, \quad (162)$$

where according to Eq. (75)  $\boldsymbol{\tau}_0 = \boldsymbol{\tau}(r=0) = 0$ .

Thus,

$$\exp\left[\boldsymbol{\tau}(\mathbf{r}) \cdot \hat{\boldsymbol{\xi}} - \frac{h}{kT}\right] \xrightarrow{\mathbf{E} \rightarrow 0} \exp(\hat{\boldsymbol{\xi}} \cdot \mathbf{A}\mathbf{r}) \cong 1 + A_{ik} \hat{\xi}_i r_k, \quad (163)$$

and

$$Z = \int_{\theta, \phi} (1 + A_{ik} \hat{\xi}_i r_k) \sin(\theta) d\theta d\phi = 4\pi + A_{ik} \int \hat{\xi}_i d\Gamma r_k = 4\pi. \quad (164)$$

~~Hence~~ Thus,

$$p(\hat{\boldsymbol{\xi}}, h) = \frac{1}{Z} \exp\left(\boldsymbol{\tau} \cdot \hat{\boldsymbol{\xi}} - \frac{h}{kT}\right) = \frac{1}{4\pi} (1 + (\mathbf{A}\mathbf{r}) \cdot \hat{\boldsymbol{\xi}}), \quad (165)$$

and by taking ~~into account~~ using Eq. (165) in Eq. (160) we obtain

$$\begin{aligned} \frac{1}{4\pi} \int \hat{\boldsymbol{\xi}} (1 + (\mathbf{A}\mathbf{r}) \cdot \hat{\boldsymbol{\xi}}) d\Gamma &= \frac{1}{4\pi} \int (\mathbf{A}\mathbf{r}) \cdot \hat{\boldsymbol{\xi}} \otimes \hat{\boldsymbol{\xi}} d\Gamma = \frac{1}{4\pi} \left(\frac{4\pi}{3} \mathbf{I}\right) \cdot (\mathbf{A}\mathbf{r}) \\ &= \frac{1}{3} (\mathbf{A}\mathbf{r}) \cdot \mathbf{I} = \frac{\mathbf{r}}{nl} \implies \mathbf{A} = \frac{3}{nl} \mathbf{I}. \end{aligned} \quad (166)$$

~~and~~ Finally, using  $\boldsymbol{\tau}(\mathbf{E} \rightarrow 0)$  gives is

$$\boldsymbol{\tau} = \mathbf{A}\mathbf{r} = \frac{3\mathbf{r}}{nl}. \quad (167)$$